



Contents lists available at ScienceDirect

Progress in Polymer Science

journal homepage: www.elsevier.com/locate/ppolymsci



Role of polymers in the design of 3D carbon nanotube-based scaffolds for biomedical applications

María C. Serrano*, María C. Gutiérrez, Francisco del Monte

Instituto de Ciencia de Materiales de Madrid (ICMM), Consejo Superior de Investigaciones Científicas (CSIC), C/ Sor Juana Inés de la Cruz 3, 28049 Madrid, Spain

ARTICLE INFO

Article history:

Received 23 May 2013

Received in revised form 3 February 2014

Accepted 11 February 2014

Available online xxx

Keywords:

Carbon nanotubes

Electrospinning

Freeze-casting

Gel formation

Polymer

Scaffold

ABSTRACT

Since pioneer works by Iijima in 1991, carbon nanotubes (CNTs) have received a great deal of attention as confirmed by the increasing number of papers in the topic. Their unique and attractive properties have made them extensively demanded materials for a wide variety of technological applications, including their promising use as scaffolds in tissue engineering. In this review, we focus on the role that polymers (both natural and synthetic) play on the fabrication of three-dimensional (3D) CNT-based scaffolds for biomedical applications, with emphasis on biocompatible fabrication strategies such as freeze-casting, electrospinning and gel formation. These 3D matrices may be an interesting and alternative platform to circumvent structural limitations and toxicity problems of bare CNTs by the use of biocompatible dispersant polymers that allow the preparation of substrates better resembling native extracellular matrices. In any case, due to the relevance of CNT toxicity in this context, we also discuss significant works concerning cell and tissue responses to CNTs in dispersion, highlighting: (1) the asbestos-like behavior of CNTs, (2) surface functionalization as a tool to reduce CNT toxicity and (3) CNT biodistribution from the blood stream and posterior excretion. In this sense, literature revision has evidenced major toxicity issues related to: (a) the inherent insolubility and tendency to aggregate of pristine CNTs, (b) the rigidity of their structures that makes them resemble asbestos, (c) the presence of residual metal impurities or amorphous carbon from their synthesis, and (d) the depletion of culture media components due to the adsorptive properties of CNTs. Nevertheless, as expected for almost any material, we also illustrate how dose plays a key role in the biological responses induced. Overall, this critic review is expected to help research community working on polymers and CNTs, as well as other carbon nanomaterials such as graphene, to identify useful guidelines that help advancing the use of 3D CNT-based scaffolds in biomedical applications.

© 2014 Elsevier Ltd. All rights reserved.

Contents

1. Introduction	00
2. 3D CNT-based scaffolds without polymers	00
3. 3D CNT-based scaffolds with polymers	00
3.1. Freeze-casting	00
3.1.1. Natural polymers	00

* Corresponding author at: Laboratory of Neural Repair and Biomaterials, Hospital Nacional de Parapléjicos, Finca de la Peraleda s/n 45071 Toledo, Spain.
Tel.: +34 925 247758; fax: +34 925 247 745.

E-mail address: mslopezterradas@sescam.jccm.es (M.C. Serrano).

3.2.	Electrospinning	00
3.2.1.	Natural polymers	00
3.2.2.	Synthetic polymers	00
3.2.3.	Blends	00
3.3.	Gel formation	00
3.3.1.	Natural polymers	00
3.3.2.	Synthetic polymers and blends	00
3.4.	CNT-coating of pre-formed scaffolds	00
3.5.	Other fabrication techniques	00
4.	Unraveling CNT toxicity	00
4.1.	Asbestos-like behavior of CNTs	00
4.2.	Surface functionalization as a tool to mitigate CNT toxicity	00
4.3.	CNT biodistribution from the blood stream and posterior excretion	00
5.	Final discussion and conclusions	00
	Acknowledgements	00
	Appendix A. Notes	00
	References	00

1. Introduction

Carbon nanotubes (CNTs) have devoted a great deal of attention in the past two decades due to their unique and attractive properties, as demonstrated by the increasing number of papers in the topic (Fig. 1). CNTs are an allotropic form of carbon defined as hollow cylinders exclusively composed of graphitic carbon sheets generally rolled as either a single- (SWCNTs), doubled- (DWCNTs) or multi-walled structure (MWCNTs) [1,2]. As nanomaterials, CNT diameter must be always comprised within the nanometer scale (0.5–2 nm for SWCNTs, *ca.* 3 nm for DWCNTs and 2–100 nm for MWCNTs), but their length easily reaches microns. The small CNTs can be rolled up in different ways, thus resulting in armchair, zigzag and chiral types [3]. Three major methods have been used for the mass production of highly purified CNTs [4]: arc-discharge [5], laser ablation [6] and chemical vapor deposition (CVD) [7], the last one being the most commonly used. CVD involves the growth of CNTs as a vertically aligned structure by using a gaseous carbon supply (hydrocarbon feedstock) and a metal catalyst (*e.g.*, nickel) at high temperatures (typically >700 °C). They can be later removed, or not, from this structure depending on the desired use [8], and then incorporated into a wide variety of composites. In regards to their attractive features, CNTs have exceptional mechanical properties, with a reported Young's modulus higher than 1 TPa and tensile strengths up to 63 GPa (10–100 times higher than steel) [9,10], and thermal stability up to 2800 °C under vacuum [11]. Electrical conductivities of 92 Scm⁻¹ have been described [12]. The exceptional mechanical, electrical and thermal properties mentioned above are caused by the sp² hybridization that maintains the carbon atoms bonded to each other in the CNT structure [1]. Other attractive properties of CNTs include: an ordered structure, lightweight, high aspect ratio, high surface area, adsorptive properties, intrinsic near-infrared optical adsorption, Raman scattering resonance, photoluminescence, and photo-acoustic properties.

Since their discovery a few decades ago [13,14], an extensive progress has been devoted to use CNTs as brick elements for the development of advanced materials

with remarkable characteristics. In this sense, the incorporation of CNTs into composite materials benefits from their mechanical, thermal and electrical properties, among others, while reducing their limitations. Particularly, the fabrication of diverse CNT-based polymer composites in the last decade has opened their use in a wide collection of applications, including flexible electrodes in displays, electronic paper, antistatic coatings, bullet-proof vests, protective clothing, and high-performance composites for aircraft and automotive industries [15,16]. More recently, CNTs have also shown utility in the emerging field of nanobiotechnology. In this context, CNTs have been already exploited for the preparation of biosensors [17–19], field emission devices [20], gas storage systems [21], tips for atomic force microscopy [22], nano-surgical needles [23], and fuel-powered artificial muscles [24], among others. In the area of tissue engineering [1,25–27], they have been extensively explored for bone regeneration [28–31], nerve tissue repair [32–36], and blood contacting materials [37,38]. Last but not least, the adsorptive properties of CNTs, along with their high aspect ratio, have encouraged their application as molecular carriers in a variety of delivery systems, including drugs, proteins, DNA, and even small interference RNA [39–46].

Despite their attractive potential, important limitations arise when using CNTs for biomedical applications. Particularly, CNT toxicity still remains as a major issue limiting their biological use [47], as well as the mechanical and structural restrictions of substrates exclusively constituted by CNTs. In an attempt to aid both aspects, polymers have been extensively explored as a more permissive and versatile platform for the integration of CNTs in biological systems. Results in this sense have permitted the fabrication of an ample repertoire of 3D architectures (*i.e.*, scaffolds), thus benefitting CNT toxicity when involving the use of biocompatible dispersant polymers. In the particular context of tissue regeneration, 3D scaffolds have been pursued to serve as matrices that resemble the geometry, chemistry and signaling environment of the natural extracellular matrix (ECM) and its role of offering structural support and a favorable environment for tissue growth and vascularization [48]. Importantly, 2D culture systems fail reproducing

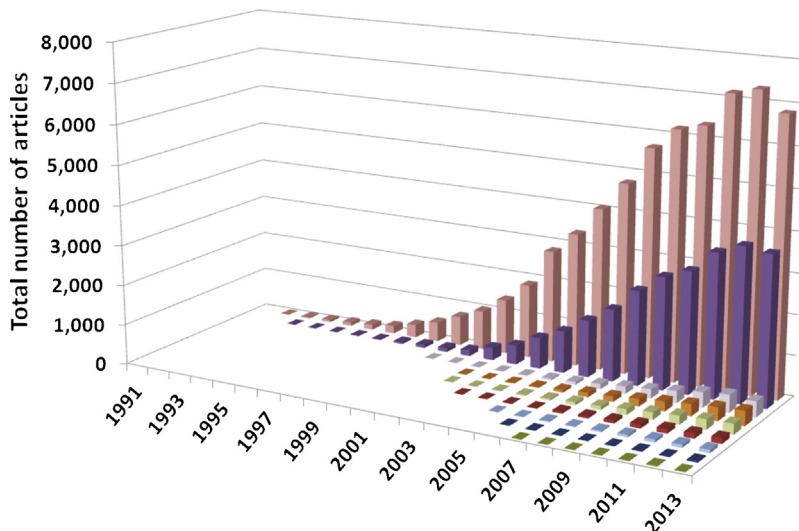


Fig. 1. Total number of articles and reviews published on the topic of CNTs since 1991 (60,713; pink bars) in comparison to those involving either the use of polymers (25,545; dark purple), an intended use in biomedical applications (2157; light purple), the preparation of scaffolds (1778; orange) or the combination of polymers in scaffolds (1298; light green). Please note the still reduced number of publications on the use of CNTs in the shape of scaffolds for either tissue engineering (681; red), biomedical applications (378; light blue), bone regeneration (89; dark blue) or nerve regeneration (62; dark green) (Please refer to Notes for further search details). (For interpretation of the references to color in this figure legend, the reader is referred to the web version of the article.)

the complex and dynamic environments of native tissues and may misrepresent findings by forcing cells to adjust to an artificial, flat and frequently rigid surface [49]. To this aim, tissue engineering efforts have prompted the development of 3D scaffolds by the use of a wide variety of strategies, mainly including hydrogel formation, polymer processing for the acquisition of stochastic architectures (e.g., freeze-casting and gas-foaming for sponge-like structures and electrospinning for fibrous ones) and more recent computer-assisted fabrication techniques such as solid free-form and 3D cell photolithographic patterning [49,50]. Approaches to this purpose should take into account features at the macro-, micro- and nano-scales to better reproduce the ECM (i.e., an intricate interwoven protein fiber meshwork embedded in a highly hydrated gel-like structure) [49]. Furthermore, the accomplishment of cell growth in these 3D structures is, by no means, a trivial goal as major spatial limitations arise including poor nutrients/oxygen availability and cellular waste product accumulation in the interior structure of the scaffolds, also evidenced by computational simulations [51].

At this stage, we would like to acknowledge some recent reviews describing 3D CNT-based architectures with applications in energy, adsorption or catalysis, among the most relevant [52]. However, while recognizing their tremendous interest, a review focusing on the most remarkable and biocompatible strategies for the fabrication of 3D polymer-CNT scaffolds with envisioned biomedical applications may be of great interest as well. Thus, in this review, we will first describe some few works on the preparation of bare 3D CNT-based scaffolds and how the polymer absence limits the utility of these scaffolds – in both structural and functional terms – in biomedical applications. Then, we will provide a full description of both the biocompatible strategies and the different polymers (both natural and

synthetic) that have been used to date for the fabrication of 3D polymer-CNT scaffolds. Finally, due to the relevance of CNT toxicity in the field of biomedicine, we will also discuss significant works concerning CNT interactions with mammalian cells and tissues. In this sense, results regarding cell and tissue responses to CNTs in dispersion are presented, with emphasis on: (1) the asbestos-like behavior of CNTs, (2) the use of surface functionalization as a tool to mitigate CNT toxicity and (3) CNT biodistribution from the blood stream and posterior excretion. Other interesting carbon-based nanomaterials, such as graphene, carbon nanofibers (CNFs), nano-horns, and nano-onions fall out of the scope of this review [1,2,26,53–57]. For further details in the use of CNTs for tissue engineering applications, readers are referred to excellent articles on the topic [1,26,35,58–65]. Thorough reviews focused on composites made of CNTs and polymers for applications other than biomedicine [66–69], as well as those centered on the specific physico-chemical benefits of this combination [16,70,71], may be also of great interest for readers.

2. 3D CNT-based scaffolds without polymers

Rare attempts have been performed to develop bare CNT-based scaffolds. For instance, Lobo and colleagues have designed structures based on vertically aligned MWCNTs by using a microwave plasma CVD process on either silicon or titanium substrates [72–74]. In a different approach, Correa-Duarte et al. developed carboxyl-functionalized MWCNT scaffolds with honeycomb-like cavities that were able to support L929 fibroblasts growth [8]. These structures were also fabricated by CVD on a silicon substrate (Nanolab Inc.). In this case, the acid solution used for functionalization created capillary and tensile forces that participated in the formation of the 3D self-assembly, as

previously reported by others [75]. By means of this technique, cavities varying from 5 to 60 μm and 5 to 15 μm in diameter were obtained by modeling MWCNTs of 50 and 35 (please insert here the symbol of microns) in length, respectively. Other interesting attempts include the fabrication of pristine CNT round islands as described by Sorkin et al. [76]. In these structures, the authors demonstrated entanglement of neural processes as a result of a neuronal anchorage mechanism to these rough surfaces (either 20 or 80 μm in diameter). Along these lines, Gabay et al. engineered self-organized neural networks as ganglion-like clusters using lithographically defined CNT islands of high density [77], with neural bridging gaps exclusively formed between neighboring islands. In more recent reports, a rope-like structure (1 mm in diameter, 1.5 cm in length) merely made of SWCNTs promoted the early neuronal differentiation of HCN-A94-2 neural stem cells synergistically with electrical stimulation (5 mV, 0.5 mA, 25 ms, intermittent stimulation) [78]. Neurites displayed higher probability of growing along the spiral topography of the rope, as previously reported on other aligned CNT-based substrates.

Careful inspection of these results allows identifying two major drawbacks regarding the use of these scaffolds for biomedical applications. First, although CNTs are known for their superior strength and mechanical properties, an important structural restriction arises when assembled into a 3D architecture merely composed of CNTs. Particularly, the absence of an agglutinant material that adsorbs external mechanical stimuli (e.g., compression, flexion or bending, among others) results in the fabrication, in most of the cases, of highly fragile substrates for tissue implantation. Besides this structural deficit, the other major concern is the induction of enhanced toxicity responses caused by the direct contact of cells and tissues with CNTs from an early stage after implantation. In this sense, CNT toxicity still remains unclear as confusing and controversial results have been reported [25,47,79]. Generally, nanomaterial-induced cytotoxicity has been related to size/mass, shape, surface charge, and functionalization [80], with both size-dependent [81–83] and composition-dependent [84] toxicity mechanisms. In the particular case of CNTs, similar findings have been shown with special attention placed on size, geometry, surface charge, and functionalization, as well as impurities of amorphous carbon and metal catalysts from their synthesis [1,85,86]. The large surface area of CNTs along with their adsorptive properties have been also considered as critical factors for inducing toxic effects, as they may promote cell death from starvation by the depletion of nutrients and growth factors in the media at doses as low as 0.01 mg mL⁻¹ [87]. Nonetheless, this aspect has been pointed out by some authors as an interesting tool to reduce their cytotoxicity as well [88]. Given the relevance of CNT toxicity in the particular context of biomedical applications, further discussion on remarkable works in the topic is included at the end of this review (see Section 4).

3. 3D CNT-based scaffolds with polymers

In order to avoid the two major restrictions of bare CNT-based scaffolds (*i.e.*, structural/mechanical deficit and

enhanced CNT toxicity), the incorporation of CNTs into polymer-based composites has arisen as an attractive strategy frequently pursued [66,68]. Attempts in this sense rely on the use of CNTs as reinforcements or additives to improve material physicochemical properties (e.g., strength, flexibility, electrical conductivity) [16,71] or to achieve new functionalities [61]. Moreover, the use of polymers also allows the accomplishment of a wider repertoire of mechanically stable scaffold structures while reducing CNT cytotoxicity in the resulting materials. A broad collection of methodologies has been explored and optimized for the preparation of 2D CNT-based composites in the form of films and fibers (e.g., solution-evaporation technique, layer-by-layer (LbL) deposition) [15,89–91]. However, the fabrication of 3D architectures has been more rarely accomplished, with some approaches including the use of natural polymers such as chitosan [92–96], porous bioglass-based foams [97], gelatin [98], silk [99], alginate [100], or collagen [101]. Furthermore, the applicability of synthetic polymers for CNT dispersion has been also exploited, including polyurethanes [29,37], nylon [38], polycarbosilane [30], poly(carbonate) urethane [102], poly(lactic-co-glycolic acid) (PLGA) [103,104], polystyrene [105], poly(methyl methacrylate) (PMMA) [106], and poly(propylene fumarate) [107], among others. Novel approaches incorporating CNTs to self-assembled aligned gels composed of charged amphiphilic molecules have been recently explored [108], with resulting composites displaying electrical conductivities in the order of 1–10 S cm⁻¹ in the dry state. For the preparation of 3D CNT-based scaffolds with controlled and interconnected porosity, methodologies such as freeze-casting and electrospinning have been applied [52]. In this section, we will expose the most relevant biocompatible methodologies described to date for the fabrication of CNT-based scaffolds with 3D architecture and potential for tissue regeneration, including the use of natural and synthetic polymers or their blends. Fig. 2 and Table 1 summarize some of the most relevant achievements in this sense.

3.1. Freeze-casting

A close inspection to the literature allows one to point to cryogenic processes as excellent candidates for the purpose of templating [109]. These processes consist of the freezing (storage in the frozen state for a certain time) and defrosting (simple thawing or freeze-drying) of low or high molecular-weight precursors, as well as colloid systems, able to form either a water solution or suspension or a hydrogel. Thus, the formation of crystalline ice (typically hexagonal ice) causes every solute originally dispersed in the aqueous medium to be expelled to the boundaries between adjacent ice crystals. Subsequent freeze-drying (high-vacuum sublimation of ice) gives rise to a cryogel, whose name derives from the Greek $\kappa\rho\iota\sigma$ (kryos) meaning frost or ice. Cryogels are macroporous structures characterized by “walls” of matter enclosing empty areas where ice crystals originally resided. The freeze-drying process also allows the achievement of monoliths that preserve the size and shape of the container submitted to freezing. Cryogels

Table 1
Examples of CNT-based scaffolds tested *in vitro* and/or *in vivo* for biomedical applications.

CNT type	Polymer	Preparation method	Pore size (μm)	Young's modulus (MPa)	Conductivity (S cm^{-1})	Application	Studies <i>in vitro</i>	Studies <i>in vivo</i> (implant location)	Reference
MWCNT	-	CVD	5–15/5–60	NR	NR	Tissue engineering	L929 fibroblasts	-	[8]
MWCNT	-	Microwave plasma CVD	-	NR	NR	Bone regeneration	Saos-2 osteoblasts	-	[72–74,199,200]
MWCNT	-	CVD	NA	NR	NR	Nerve regeneration	L929 fibroblasts	-	[76]
MWCNT	-	CVD	NA	NR	NR	Nerve regeneration	embryonic fibroblasts	-	[77]
MWCNT	-	CVD/wound into ropes	NA	NR	NR	Nerve regeneration	Rat cortical and hippocampal cells	-	[78]
MWCNT	CHI	Freeze-casting	14 (width)	5.2	1.7	Bone regeneration	Rat cortical cultures	-	[93]
MWCNT	CHI	Freeze-casting	14–63	1–5	0–2	Tissue engineering	HCN-A94-2 neural stem cells	Ectopic bone formation in muscle (mouse)	[120]
CS			9	5–7	0–2		C2C12 cells	-	
Gelatin			6–7	8–12	0.05		L929 fibroblasts	-	
MWCNT	CHI	Freeze-casting	46–200	NR	NR	Bone regeneration	Saos-2 osteoblasts	-	[121,122]
MWCNT	Collagen I	Freeze-casting	-	NR	NR	Bone regeneration	EC _{PC} cells	-	[125]
MWCNT	CHI	Freeze-casting	e.g., 16	NR	3.7	Bone regeneration	MG-63 cells	Ectopic bone formation in muscle (mouse)	[96]
SWCNT	CA	Electrospinning	-	-	NR	Biofuel cell electrode	-	-	[132]
SWCNT	CHI/PVA	Electrospinning	<4	Up to 22.5 (tensile stress)	NR	Vascular regeneration	HUVEC (abdominal aorta)	-	[151]
SWCNT	Agarose	Electrospinning	NA	Up to 1280 (tensile modulus)	3–191	Nerve regeneration	hBDC U373-MG	Rat cerebral cortex implantation	[130]
MWCNT	PCL	Electrospinning	$\ll 10^b$ disordered	ca. 18	-	Anti-cancer drug release	Primary astrocytes	Normal and tumor cells	[140]
MWCNT	PLA	Electrospinning	$\ll 10^b$ disordered or aligned	ca. 18	10^3 – 10^4 ($\Omega \text{ square}^{-1}$)	Bone regeneration	Osteoblasts	-	[139]
MWCNT	PLGA	Electrospinning/knitting	$\ll 10^b$	8% (extension to break)	0.90–1.01 $\text{k}\Omega \text{ cm}^{-1}$	Tissue engineering	NR6 fibroblasts	-	[165]
MWCNT	PA/P(NIPAM-co-MAA)	Electrospinning	<15 ^b	NR	NR	Tissue engineering	L929 fibroblasts	-	[134]
MWCNT	PLCL	Electrospinning	NR	NR	NR	Nerve regeneration	PC-12 cells	-	[143,144]
MWCNT	PCL/PAA/PVA	Electrospinning	<10 ^b	7.1–12.5	0.028–0.046	Muscle tissue engineering	DRG neurons	-	[141,142]
MWCNT	PVA/CHI	Electrospinning	<5 ^b	81–159	NR	Tissue engineering	Primary muscle cells	-	[150]
MWCNT	PU	Electrospinning	$\ll 5^b$	NR	NR	Tissue engineering	L929 fibroblasts	-	[148]
							3T3-L1 fibroblasts	-	
							endothelial cells	-	

Table 1 (Continued)

CNT type	Polymer	Preparation method	Pore size (μm)	Young's modulus (MPa)	Conductivity (S cm^{-1})	Application	Studies <i>in vitro</i>	Studies <i>in vivo</i> (implant location)	Reference
SWCNT/MWCNT	PLLA	Electrospinning	~2	NR	5–6 mS cm^{-1}	Nerve regeneration	mESC	–	[145]
MWCNT	CA/CHI	Electrospinning/LbL	<10 ^b	36–70	NR	Tissue engineering	L929 fibroblasts	–	[162]
SWCNT	PLLA	Phase-separation	103	12.5	NR	Bone regeneration	Rat bone marrow cells	–	[173]
SWCNT	PLGA	Solution evaporation	–	–	–	Magnetic resonance	–	Subcutaneous (rat)	[215]
SWCNT	Vacuum drying	–	–	–	–	–	–	–	–
SWCNT	Collagen	Gel formation	<2 ^b	NR	NR	Tissue engineering	SMC	–	[152]
SWCNT	Collagen	Gel formation	–	NR	NR	Tissue engineering	PC12 cells and 3T3 fibroblasts	–	[153]
SWCNT	Collagen	Gel formation	≤1	3–4 kPa ^c	NR	Tissue engineering	Endothelial cells	–	[154]
SWCNT	Collagen/matrikel	Gel formation	NA	NR	287–666	Nerve regeneration	Schwann cells	–	[156]
SWCNT	Alginate	Gel formation/freeze-casting	100–200	NR	NR	Tissue engineering	MG-63 osteoblasts	Subcutaneous (rat)	[128]
SWCNT	Alginate	Gel formation/LbL	500	0.4–1.4	NR	Tissue engineering	Rat heart endothelial cells	–	[100]
MWCNT	Methacrylate/gelatin	Gel formation	5–50 ^b	60 kPa (elastic) 30 kPa (compression)	NR	Tissue engineering	NIH-3T3 hMSC	–	[98]
MWCNT	Silk	Gel formation	NA	NR	NR	Nerve regeneration	Human H9 ESC	–	[157]
MWCNT	PCL	Solution evaporation	–	85–110 (tensile) 345–400 (compression)	NR	Bone regeneration	Rat BMSC	–	[170]
SWCNT	PPF	Particulate leaching	40–100	Up to 0.7	NR	Bone regeneration	Rat BMSC	Femur condyle and subcutaneous (rabbit)	[171]
MWCNT	P(3HB)	Solvent casting and particulate leaching	100–200	NR	NR	Bone regeneration	MG-63 cells ^a	Subcutaneous ^a	[169]
MWCNT	PLGA	Solvent casting	–	248–375	NR	Bone regeneration	MSC	–	[166]
MWCNT	Collagen (AteloCell®)	Coating	200–400	NR	NR	Bone regeneration	Primary osteoblasts	Bone	[101,161]
MWCNT	PET/gelatin	Coating	60–150	NR	NR	Nerve regeneration	Mouse D3 ESC Transgenic mouse ESC	–	[163]

BMSC, bone marrow-derived stroma cells; CA, cellulose acetate; CHI, chitosan; CNT, carbon nanotubes; CS, chondroitin sulfate; CVD, chemical vapor deposition; DRG, dorsal root ganglion; EC_{PC}, endothelial cells derived from peripheral progenitors; ESC, embryonic stem cells; hBDC, human brain-derived cells; HUVEC, human umbilical vein endothelial cells; LbL, layer-by-layer deposition technique; mESC, mouse embryonic stem cells; MSC, mesenchymal stem cells; MWCNT, multi-walled carbon nanotubes; PA, polyaniline; PAA, poly(acrylic acid); P(3HB), poly(3-hydroxybutyrate); PCL, polycaprolactone; P(NIPAM-co-MAA), poly(*N*-isopropyl acrylamide-co-methacrylic acid); PLA, poly(DL-lactic acid); PET, poly(ethylene terephthalate); PLGA, poly(lactide-co-glycolide); PLCL, poly(L-lactic acid-co-3-caprolactone); PLLA, poly(L-lactic acid); PPF, poly(propylene fumarate); PU, polyurethane; PVA, poly(vinyl alcohol); SMC, smooth muscle cells; SWCNT, single-walled carbon nanotubes; NA, not applicable; NR, values not reported.

^a Studies not performed with the CNT-containing matrices.

^b Values estimated from SEM images.

^c Average static modulus at 15% strain and low loading level.

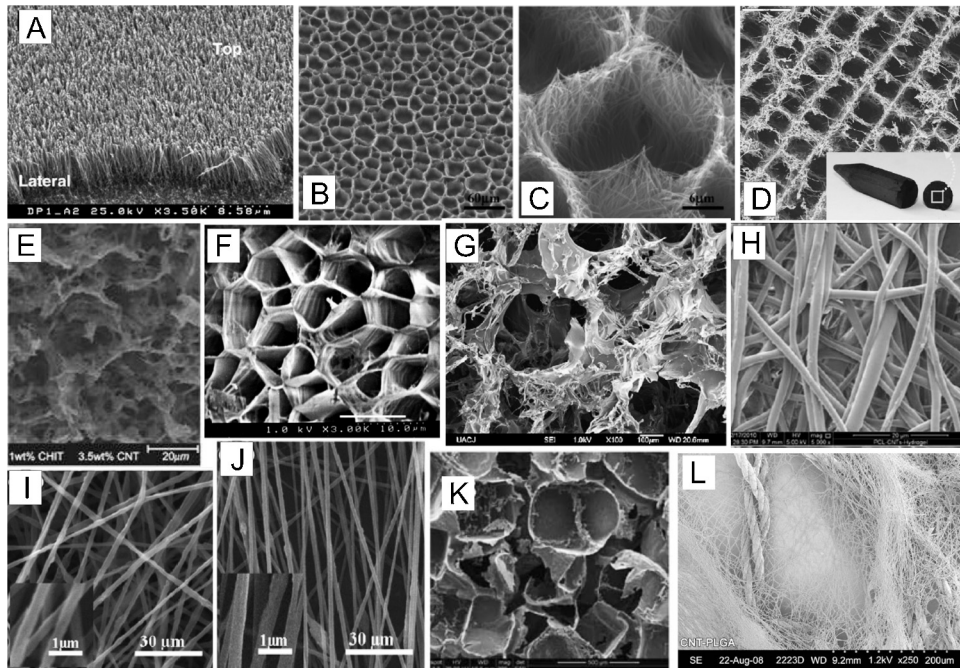


Fig. 2. SEM images illustrating exemplary 3D architectures of CNT-based materials obtained by the use of diverse fabrication techniques: (A) MWCNT films by CVD [74], Copyright 2008, Reproduced with permission from Elsevier Ltd; (B and C) bare CNT-based networks by CVD and posterior use of chemically induced capillary forces [8], Copyright 2004, Reproduced with permission from the American Chemical Society; (D) porous 3D chitosan/MWCNT scaffolds by ISISA process; [93], Copyright 2008, Reproduced with permission from Elsevier Ltd; (E) freeze-casted chitosan/MWCNT scaffolds [96], Copyright 2008, Reproduced with permission from the American Chemical Society; (F) lyophilized hyaluronic acid hydrogels reinforced with SWCNTs [126], Copyright 2008, Reproduced with permission from the American Chemical Society; (G) porous chitosan scaffolds prepared by thermal-induced phase separation and loaded with 1 wt% MWCNTs [92], Copyright 2010, Reproduced with permission from Elsevier Ltd; (H) electrospun polycaprolactone/MWCNT/poly(acrylic acid)/poly(vinyl alcohol) scaffolds at 5000× [142], Copyright 2011, Reproduced with permission from John Wiley and Sons.; (I and J) random-oriented and aligned electrospun PLA/MWCNT nanofiber meshes [139], Copyright 2011, Reproduced with permission from Elsevier Ltd; (K) highly porous scaffolds made of a dodecylated ultra-short SWCNT nanocomposite by a thermal-crosslinking particulate-leaching technique (scale bar 500 μm) [171], Copyright 2007, Reproduced with permission from Elsevier Ltd; (L) tubular knitted scaffolds from a 9 ply MWCNT yarn and electrospun PLGA nanofibers [165], Copyright 2009, Reproduced with permission from Elsevier Ltd.

of polymeric nature were first reported more than 40 years ago [110,111], and their properties, rather unusual for polymer gels, soon attracted attention. Since then, polymer cryogels of many different compositions (e.g., poly(L-lactic acid)(PLLA) and PLGA [112,113], gelatin [114], gamma-poly(glycolic acid)/chitosan [115,116], collagen and elastin [117], collagen-glycosaminoglycan [118], or albumin-cross-linked polyvinylpyrrolidone [119], among others) have been widely used in biomedicine (e.g., for tissue engineering and drug delivery purposes), most likely because of the biocompatible character of both the fabrication process and the precursors. It is noted that the synthesis starts from an aqueous solution, suspension or hydrogel and proceeds in the absence of further chemical reactions or purification procedures, thus avoiding potential medical complications which might be associated with the presence of byproducts and/or the removal of templates.

3.1.1. Natural polymers

Within the context of freeze-casting methods, we have recently reported on the use of the ISISA process (ice segregation-induced self-assembly), which basically consists of a unidirectional freezing of the sample by dipping it into a liquid nitrogen bath at a constant rate, followed by

freeze-drying. In this case, unidirectional freezing allowed the achievement of macroporous structures with well-aligned microchannels in the freezing direction and a well-patterned morphology between channels (e.g., lamellar and micro-honeycomb, respectively). The application of the ISISA technique to a dispersion of HNO₃-treated MWCNTs (up to 8 wt%) in an aqueous solution of chitosan (1 wt%) allowed the fabrication of MWCNT-based 3D scaffolds useful in bone tissue regeneration [93,94]. By means of this procedure, the resulting 3D structures contained up to 89 wt% of MWCNTs, a percentage way higher than any other previously reported (typically below 5 wt%). In these scaffolds, good conductivity values for biomedical applications were achieved (e.g., 2.5 S cm⁻¹) thanks to an adequate interconnection among CNTs that guaranteed an efficient charge transfer. After loading of recombinant human bone morphogenetic protein 2 (rhBMP-2) and implantation in subcutaneous pockets in mice, these materials promoted ectopic bone formation (Fig. 3) [93]. When homogeneously mineralized by a “flow-through” electrodeposition process (Fig. 4), these scaffolds were also able to enhance osteoblast terminal differentiation [95]. The application of the ISISA methodology has allowed the successful preparation of 3D biocompatible CNT-based scaffolds with other biopolymers as well, such as chondroitin sulfate and

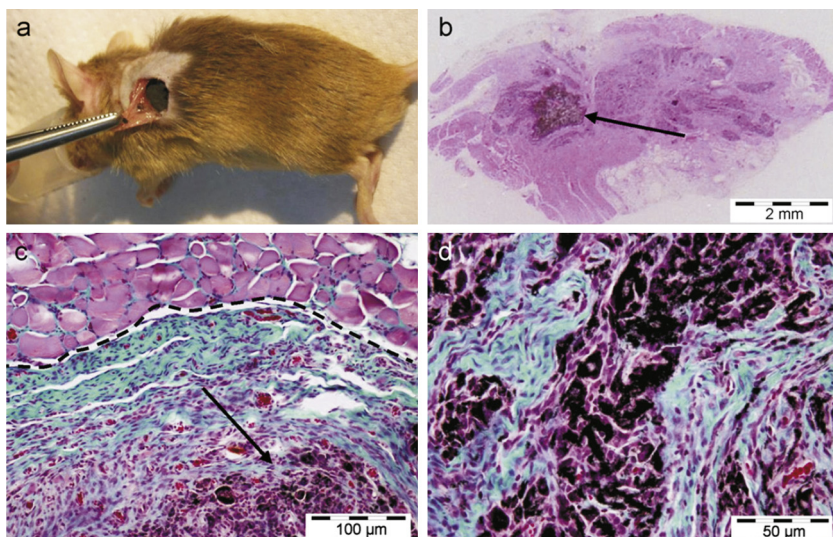


Fig. 3. Picture (a) shows the surgery implantation of rhBMP-2 adsorbed MWCNT/chitosan scaffolds into a mouse subcutaneous muscular pocket. Optical microscope micrograph (b) shows regenerated bone tissue and a minor fraction of the remaining scaffold. Optical micrograph (c) shows a detail of regenerated bone tissue (collagen-expressing cells, blue-green colored) after major disassembly of the scaffold, surrounded by muscle tissue (pink colored). Optical micrograph (d) shows a detail of remaining scaffold plenty of fibroblasts (purple colored), prior to its disassembly and colonization by collagen-expressing cells [93]. Copyright 2008, Reproduced with permission from Elsevier Ltd. (For interpretation of the references to color in this figure legend, the reader is referred to the web version of the article.)

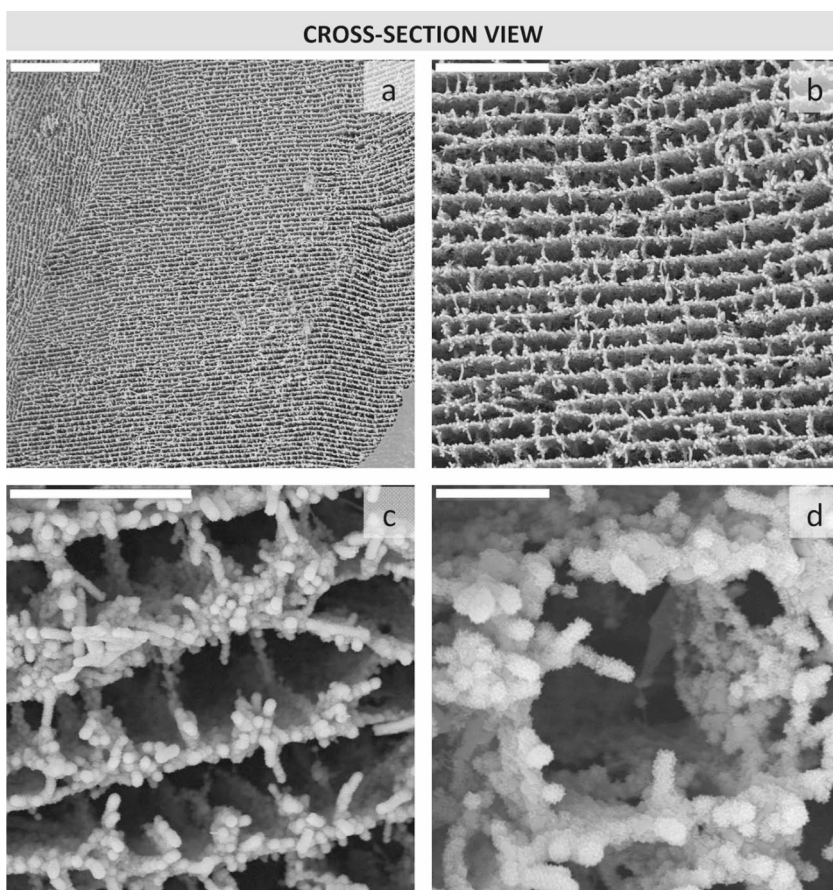


Fig. 4. SEM micrographs of MWCNT/chitosan scaffolds after mineralization in flow-through conditions revealing the long-range homogeneity of the mineral coating across the entire scaffold structure. Electrodeposition was carried out over 30 min at 30 °C and 1.4 V. Scale bars represent 200 µm (a), 50 µm (b), 20 µm (c), and 5 µm (d) [95]. Copyright 2012, Reproduced with permission from John Wiley and Sons.

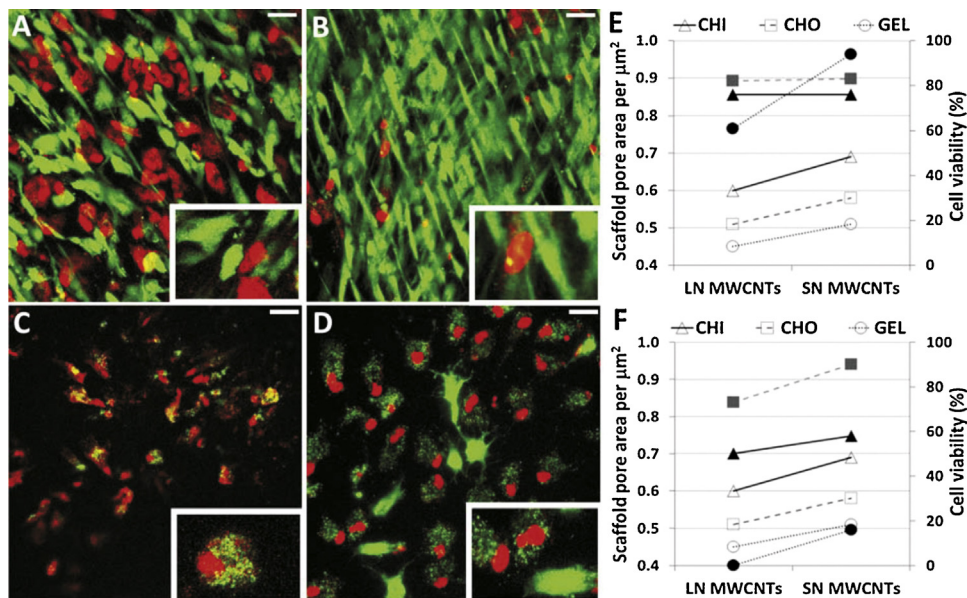


Fig. 5. Cell viability studies on endothelial cells derived from peripheral progenitors (EC_{PC}) cultured on 3D CNT-based scaffolds containing either chondroitin sulfate (A and B) or gelatin (C and D) as polymer dispersants. In these scaffolds, two types of MWCNTs were tested: acid-treated (A and C) and double-acid-treated (B and D). In the images, alive cells appear stained in green while dead cells do in red. Details of stained cells are included as insets. Scale bars: 25 μm . (E and F) Correlation between scaffold topography, measured as pore area per μm^2 (open labels, left Y axis), and cell viability (filled labels, right Y axis) on Saos-2 osteoblasts (E) and EC_{PC} (F) cultures. Effects caused by the use of different polymers (i.e., CHI, chitosan, CHO, chondroitin sulfate and GEL, gelatin) and two types of CNTs: acid treated MWCNTs (LN) or double-acid-treated MWCNTs (SN) [120]. Copyright 2013, Reproduced with permission from the Royal Society of Chemistry. (For interpretation of the references to color in this figure legend, the reader is referred to the web version of the article.)

gelatin, thus allowing the achievement of 3D substrates with different architectural and morphological features at the microscale [120]. We then explored the interaction of these scaffolds with three types of mammalian cells displaying different size and adhesion pattern. Interestingly, scaffolds with both a pore size in range with that of cells and lower surface roughness revealed the highest viability values. On the contrary, those with a smaller pore size and higher surface roughness accounted for the lowest cytocompatibility (Fig. 5). These findings clearly demonstrate how varying scaffold-dependent parameters in accordance to those of target cells benefits the fabrication of optimized biomaterials for biomedical applications. Lau et al. also developed conductive, macroporous composite scaffolds made of chitosan (1 wt%) and MWCNTs (20–30 nm in diameter, 10–30 μm in length, up to 5 wt% in the original dispersion, 95 vol% in the final precipitate) [96]. A controlled cooling at -20°C under 8 min was applied to these solutions, with a resulting multidirectional porosity of 97% and both a macro- and mesoporous distribution of pores. A mean pore size of 16 μm was obtained for scaffolds containing 1 wt% of chitosan and 2.5 wt% of CNTs, which was evidenced as the optimal threshold concentration of CNTs for good conductivity performance (volume resistivity of 3.7 $\Omega \text{ cm}$).

By using a fast, non-directional freezing method, Venkatesan et al. fabricated 3D chitosan scaffolds containing MWCNTs (<8 nm in diameter, 10–30 μm in length) for bone tissue engineering applications [121]. In this case, well-dispersed aqueous mixtures of chitosan, hydroxyapatite and carboxyl-functionalized MWCNTs were pipetted in cell culture plates, frozen at -80°C for 5 h and,

subsequently, freeze-dried. The resulting scaffolds were treated with a NaOH solution (10 wt%) for 24 h and finally rinsed in water until the pH became neutral. In this case, porosity values of 87% were obtained, with a non-ordered porous structure resulting from the non-controlled freezing method applied. In more recent studies [122], these authors demonstrated the existence of chemical interactions between the amide groups in chitosan and the carboxylic groups in functionalized MWCNTs when preparing these scaffolds with low- and high-molecular weight chitosan and different amounts of MWCNTs (0.0025, 0.005 and 0.01 wt%). Additional studies with MG-63 cells (a human osteosarcoma cell line) revealed an enhanced alkaline phosphatase activity and mineralization in the presence of CNTs. In a different approach, Wallace and colleagues also used the freeze-casting technique to fabricate conductive, highly porous chitosan scaffolds containing SWCNTs (0.125–0.750 w/v%) [123]. Poly(2-methoxyaniline-5-sulfonic acid) (0.1 and 0.75 w/v%) was added to the mixture to slow down scaffold degradation. For instance, scaffolds containing 1 w/v% of chitosan and 0.25 w/v% of SWCNTs displayed a pore size of 174 μm , a compressive Young modulus of 333 kPa and resistance values of 100 Ω . In this case, the interconnected porosity obtained was found independent from composition, but dependent on the freezing temperature applied as also reported by other authors [124]. More recently, Olivas-Armendáriz et al. used this technique to fabricate chitosan/MWCNT composite scaffolds for tissue engineering with porosities as high as 92% [92]. Percentages of 0.5, 1 and 2 wt% of carboxyl-functionalized MWCNTs were

dispersed in chitosan solutions, which were subsequently frozen at -40°C and freeze-dried. A pore size ranging from 100 to 300 μm was attained. Increases in Young's modulus of 100 and 300% were reported for those scaffolds containing 0.5 and 1 wt% MWCNTs, respectively.

Other biopolymers different from chitosan, chondroitin sulfate and gelatin have been also used for the preparation of 3D scaffolds by freeze-casting. For instance, Usui et al. prepared collagen/MWCNT scaffolds containing rhBMP-2 [125]. In this particular approach, a solution with rhBMP-2 (1 $\mu\text{g mL}^{-1}$), glutamic acid, glycine, sucrose, NaCl, and Tween 80 was mixed with that containing MWCNTs (80 nm in diameter, 10–20 μm in length) and type I collagen. The resulting aqueous mixture was then lyophilized and compressed to form the 3D matrices. When implanted *in vivo*, a good bone tissue response was observed with evidences of bone repair and integration. Unfortunately, further details on their structure are missing in this article, so it is difficult to compare them with other existing scaffolds in terms of pore size or architectural pattern. In a different study, Bhattacharyya et al. reinforced hyaluronic acid hydrogels by incorporating SWCNTs (2 wt%) [126], thus resulting in a 300% increase in the dynamic mechanical properties of the composite hydrogels. After freeze-drying, the morphology of the CNT-containing gels changed significantly with respect to those without CNTs, but the swelling behavior remained unaltered. In a different approach, Kwon et al. fabricated organic silk fibroin cryogels containing MWCNTs through a sol-gel process followed by freeze-drying [127]. As reported by others [128], the presence of MWCNTs accelerated gel formation in a concentration-dependent fashion. In this case, the tridimensionality of the resulting porous scaffolds relied on the formation of a silk fibroin network and their proportion of micro- and mesopores was favored by the presence of an adequate amount of MWCNTs. In a different study, Thongprachan et al. prepared macroporous solid foams made of MWCNTs (13–16 nm in diameter, 1 to $>10 \mu\text{m}$ in length) by using a surfactant solution containing carboxymethyl cellulose sodium salt and the freeze-drying technique [129]. These authors confirmed that faster cooling rates yielded to higher structure homogeneity and smaller macropore sizes, also obtained by increasing the amount of either surfactant (0.5, 1 and 2 wt%) or CNTs (0.5, 1 and 1.5 wt%). The controlled freezing method used in this study allowed the formation of a more ordered architecture in the resulting scaffolds, with pore sizes ranging from 49 to 73 μm , which could serve in gas sensing applications.

3.2. Electrospinning

Electrospinning is an attractive technique that allows the preparation of nanofibers with a wide variety of compositions and dimensions and ability to form 3D scaffolds. In this sense, CNTs have been extensively incorporated into electrospun composite fibers.

3.2.1. Natural polymers

Ayutsede et al. fabricated nanocomposite silk fibers with SWCNTs embedded by dispersion in a solution containing formic acid and regenerated *Bombyx mori* silk

fibroin [99]. These fibers showed an increase in Young's modulus of 460% as a result of CNT reinforcement. In a different study, hybrid SWCNT/agarose fibers were made by both wet spinning and hollow-tube molding and later functionalized with laminin [130]. These composites were able to support viable primary astrocyte cultures *in vitro*, although a mild gliosis was found when some of these fibers were implanted *in vivo* in the rat cerebral cortex. Interestingly, those fibers functionalized with laminin showed a greater superficial attachment of both neurons and astrocytes (Fig. 6). In more recent reports, electrospinning has been used for the fabrication of fibrous nanocomposite scaffolds made of Zein, a well-known plant protein, and SWCNTs (up to 1 wt%) [131]. Fiber diameters ranged from 100 to 300 nm. SWCNTs have been also incorporated into electrospun scaffolds composed of cellulose acetate [132].

3.2.2. Synthetic polymers

The use of SWCNTs in combination with synthetic polymers for the fabrication of electrospun scaffolds with biomedical applicability has been more rarely accomplished, with some attempts reporting their incorporation into nanofibers of either poly(ϵ -caprolactone) (PCL) or PMMA (6 wt%) [133]. On the contrary, the use of MWCNTs has been more extensively pursued. For instance, Sharma et al. developed conducting nanofiber-based scaffolds composed of polyaniline, poly(*N*-isopropyl acrylamide-co-methacrylic acid) and MWCNTs (20–40 nm in diameter, 1–2 μm in length) [134]. Although the resulting composite fibers had an average diameter of 500–600 nm, no dimensions for the scaffold fabricated were reported, thus making difficult to elucidate the suitability of these fibers for the preparation of real 3D tissue engineering scaffolds. Chen and co-workers developed composite scaffolds by electrospinning a solution of PLGA and functionalized MWCNTs (8–15 nm in diameter, 0.5–2 μm in length, 1.5 w/v%) [103,135,136]. The averaged fiber diameter was typically around 2.15 μm , with a pore size over 10 μm , as estimated from SEM images. These authors also introduced MWCNTs into electrospun polyacrylonitrile [137]. PLGA has been used by other authors for similar purposes [138]. In more recent studies, carboxyl-functionalized MWCNTs (10–20 nm in diameter, 10–20 μm in length) were embedded into poly-DL-lactide nanofiber meshes prepared by electrospinning [139]. Percentages of CNTs from 1 to 5 wt% were incorporated and two types of configurations investigated: randomly distributed and aligned. Porosities ranged from 89 to 96%, but pore sizes were in the order of a few microns in the best cases. Electrostimulation studies of osteoblasts grown on these conductive meshes revealed cellular alignment along the electrical field direction in response to direct currents of 100 μA . In further interesting studies, this technology was applied to the fabrication of PCL/MWCNT composite nanofibers with the ability to release green tea polyphenols [140]. Freeman and colleagues have also published on the incorporation of MWCNTs (up to 0.14 wt%) in electrospun scaffolds composed of PCL and poly(acrylic acid)/poly(vinyl alcohol) (PAA/PVA) (averaged fiber diameter of 1.8 μm) [141]. The resulting fibers showed actuation after electrical

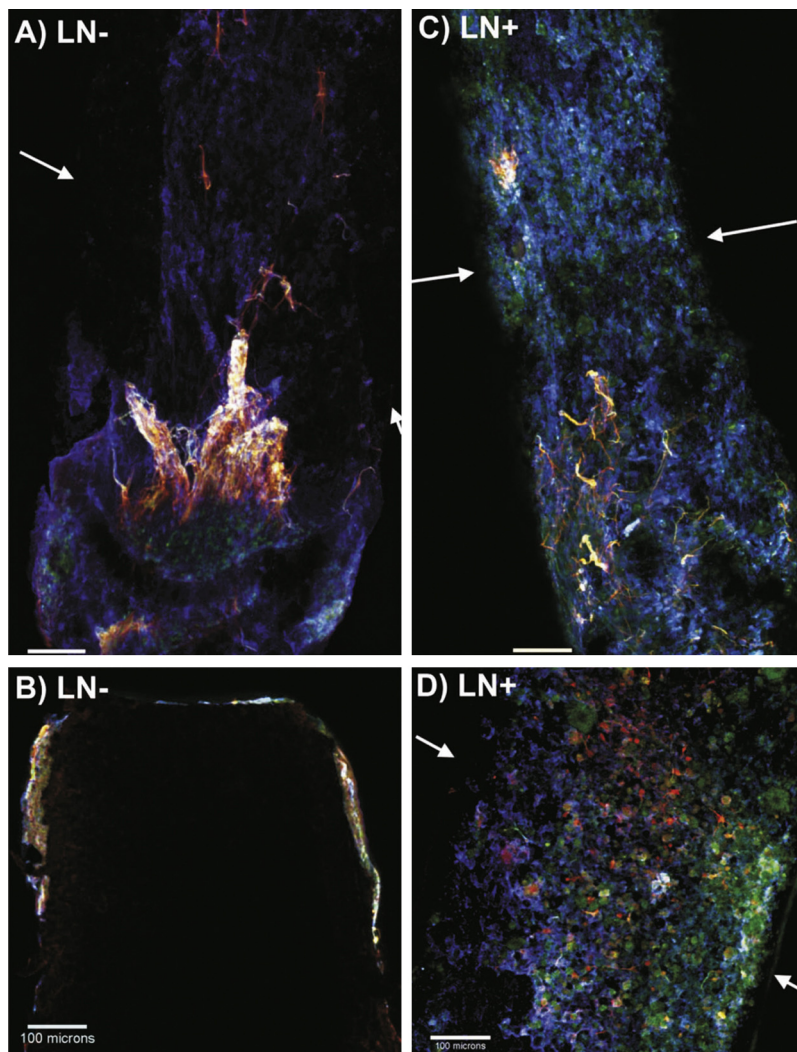


Fig. 6. Projection confocal images of fibers extracted from brains. Both sides of each fiber were mounted on the glass slide (left and right, respectively). In the images: astrocytes appear in yellow (GFAP), microglia in blue (Iba-1) and neurons in green (Nissl). Image of the laminin-functionalized fiber (LN+, C and D) demonstrates a greater attachment of all cell types when compared to non-functionalized fiber (LN-, A and B). Scale bar: 100 μm [130]. Copyright 2011, Reproduced with permission from John Wiley and Sons. (For interpretation of the references to color in this figure legend, the reader is referred to the web version of the article.)

stimulation with 15 and 20V, thus indicating their potential use as nano-actuators for skeletal muscle [142].

Concerning nerve tissue repair, Jin et al. showed an enhanced adhesion, proliferation and neurite outgrowth of PC-12 cells when cultured on MWCNT-coated electrospun poly(lactide-*co*-3-caprolactone) nanofiber scaffolds [143]. This aligned substrate has also demonstrated increased neurite length in dorsal root ganglion neurons cultured for up to 9 days [144]. More recently, Kabiri et al. reported PLLA fiber scaffolds containing CNTs as potential candidates for neural tissue regeneration [145]. These scaffolds, fabricated by electrospinning a PLLA solution supplemented with either SWCNTs or MWCNTs (3 wt% respect to polymer content), promoted cell alignment and differentiation of mouse embryonic stem cells into mature neurons (positive map-2 expression). Additionally, MWCNTs have been incorporated into porous electrospun nanofiber mats

composed of poly(ethylene oxide) [146,147]. There, authors suggested 1 wt% of MWCNT content as optimal for the enhancement of the mechanical and electrical properties of the resulting nanofibers. In a different study, Meng et al. used polyurethane (PU) as the polymer of choice to fabricate functionalized MWCNT-containing electrospun nanofibers (300–500 nm in diameter) for tissue engineering scaffolds [148]. Other polymers such as polyamide 6 have been also used for the incorporation of MWCNTs into electrospun nanofibers [149].

3.2.3. Blends

Some reports exist evolving the simultaneous use of natural and synthetic polymers. In this sense, Shi and colleagues incorporated MWCNTs (30–70 nm in diameter, 100–400 nm in length) into electrospun PVA/chitosan nanofibers for the preparation of fibrous mats [150].

The resulting matrices displayed fibers with 157 nm in diameter, porosities of 57–58% and pore sizes below a few microns. Counterpart electrospun scaffolds containing SWCNTs (up to 17 wt%) have shown also promise for neural regeneration, as they support proper growth and integration of both U373 and human brain-derived cells [151].

3.3. Gel formation

3.3.1. Natural polymers

Natural polymers such as collagen and alginate have been more extensively explored than synthetic ones for the preparation of CNT-containing hydrogels. For instance, MacDonald et al. reported on the fabrication of SWCNT/collagen composite scaffolds by means of collagen fiber gelation in response to NaOH-based neutralization and thermal treatment at 37 °C [152]. Amounts of 0.2, 0.4, 0.8, and 2.0 wt% of carboxyl-functionalized SWCNTs were incorporated into the matrices. To achieve 3D cellular colonization of the scaffold, smooth muscle cells were incorporated directly during gel formation. Crouzier et al. used a similar methodology for the preparation of collagen hydrogels with a higher content of SWCNTs (5 wt%) [153]. Additional studies by Tan et al. revealed that covalently functionalized CNTs induced the formation of larger fibril bundles by strongly binding to collagen molecules when incorporated into 3D collagen fiber-based constructs [154]. SWCNTs have also shown enhancement of PC-12 cell proliferation when dispersed in collagen hydrogels [155]. When considering glial cell behavior, interesting findings by Behan et al. evidenced different Schwann cell behavior on either 2D or 3D collagen I/matrigel hydrogels containing carboxyl-functionalized SWCNTs (10–50 µg mL⁻¹) [156]. Particularly, 2D substrates inhibited proliferation without affecting cell viability and induced morphological and metabolic changes. Neither of these effects was detected when the cells were grown on the 3D matrices.

Biocompatible alginate hydrogels containing carboxyl-functionalized SWCNTs have been also reported [128]. In these studies, the incorporation of CNTs into the gels decreased the gelation point and increased the mechanical strength when compared to conventional alginate gels. Additionally, this polysaccharide has been used to fabricate 3D scaffolds (10 mm × 10 mm × 2 mm) with SWCNTs (1%, w/w) by a free-form, computer-assisted fabrication technique [100]. By means of a multi-nozzle deposition system, LbL deposition of the gel solution allowed the acquisition of a pre-defined porous 3D structure (*ca.* 500 µm of pore size). Rat heart endothelial cells adhered, grew and remained viable on these substrates. Silk, another natural polymer, has been also successfully used for the fabrication of laminin-coated 3D composites containing MWCNTs [157]. H9 human embryonic stem cells cultured on these scaffolds expressed higher levels of β-tubulin III and nestin proteins, as indicators of neural differentiation, with enhancement of axonal length and density in this 3D structure.

3.3.2. Synthetic polymers and blends

In a different approach involving the use of synthetic polymers, ultralight MWCNT aerogels were fabricated

with a macroporous honeycomb structure defined by parallel voids of 50–150 µm and separation walls of less than 100 nm in thickness [158]. Briefly, poly(3-(trimethoxysilyl)propyl methacrylate) (PTMSPMA) was used to both disperse and functionalize the CNTs. Subsequent hydrolysis and condensation of PTMSPMA resulted in strong and permanent chemical bonding between MWCNTs that permitted the mechanical stability of the resulting conductive aerogel. Finally, although rare, some approaches have included the use of methacrylate in combination with gelatin for the preparation of blended hydrogels reinforced with MWCNTs [98]. When NIH-3T3 and human mesenchymal stem cells were encapsulated inside these 3D hybrid structures, adequate cellular adhesion and proliferation were observed.

3.4. CNT-coating of pre-formed scaffolds

Other approach to achieve CNT-containing 3D structures involves coating the surface of pre-formed 3D scaffolds of diverse composition, by means of techniques such as LbL deposition [159] or electrophoretic deposition [160], and being both natural and synthetic polymers equally explored. Regarding the use of natural ones, Hirata et al. prepared collagen sponges (AteloCell®, 9 mm in diameter, 2 mm in thickness, Koken Co., Japan) coated with MWCNTs (10–20 nm in diameter, 1–5 µm in length) for bone tissue engineering [161]. The resulting sponge was composed of a collagen membrane (1 µm in thickness) that maintained its parallel pores (200–400 µm in diameter) after soaking into an MWCNT dispersion (1 µg mL⁻¹). *In vitro* 3D dynamic flow culture conditions enhanced the differentiation of rat primary calvariae osteoblasts. Furthermore, *in vivo* implantation in the femur showed new bone formation around the scaffolds (at 28 and 56 days) and into their pores (at 28 days) [101]. In a different approach, chitosan and MWCNTs were deposited on top of electrospun cellulose acetate nanofibers via LbL deposition (averaged fiber diameter of 305 nm) to serve as a scaffold for tissue engineering applications [162]. The resulting 3D fibrous scaffolds enhanced their mechanical properties by the incorporation of CNTs. Unfortunately, uneven formation of chitosan/MWCNT clusters was observed on the fiber surface after more than 5.5 bilayers, thus significantly increasing surface roughness. With respect to the use of synthetic polymers, Zang and Yang demonstrated enhancement of neuronal differentiation of mouse embryonic stem cells cultured on MWCNT-coated 3D fibrous poly(ethylene terephthalate) (PET) scaffolds (20 µm fiber diameter, 60–150 µm pore size, 90% porosity) [163], with more neurite outgrowth and branching involving the formation of both extensive neural networks around the fibers and neurite bridges between them (Fig. 7).

3.5. Other fabrication techniques

Freeze extraction has been used for the fabrication of porous composite scaffolds containing PLLA and MWCNTs [164]. These structures showed more than 80% of interconnected porosity and pore sizes ranging from 50 to 150 µm. MWCNT yarns with 3D structure have been also achieved

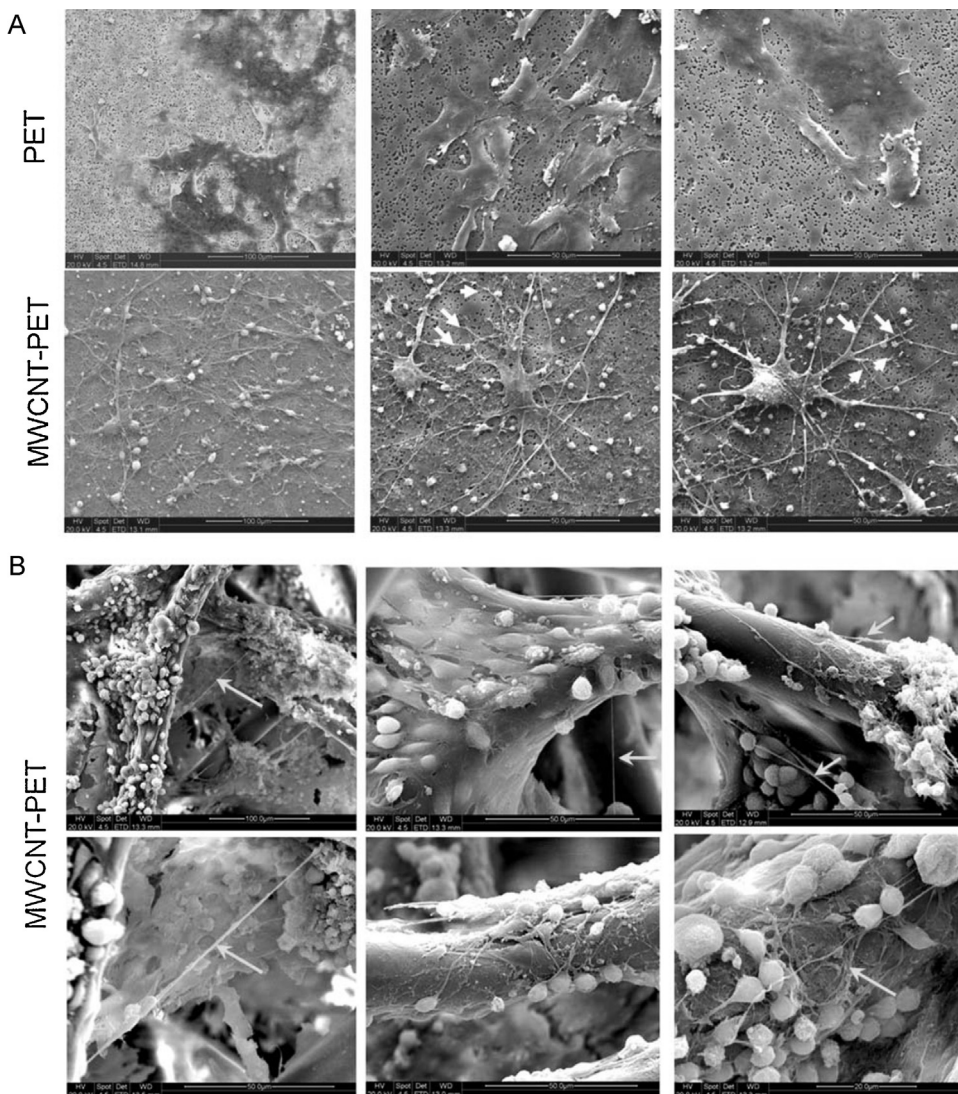


Fig. 7. SEM images showing cell morphologies of mouse embryonic stem cells after neuronal differentiation in (A) 2-D PET scaffolds with and without MWCNT coating and (B) 3-D PET scaffolds with MWCNT coating. Arrows indicate neurite fibers [163]. Copyright 2013, Reproduced with permission from the Royal Society of Chemistry.

by knitting a CNT forest obtained by CVD [165]. Briefly, MWCNTs were simultaneously drawn from a forest and twist inserted (typically 80,000 turns per meter) to form a single ply yarn. Nine single yarns were then over-twisted to obtain the 9-ply yarn that was knitted into a tubular structure by using a five needle circular weft knitting machine. Unfortunately, a glass rod was needed in the center of the knitted tube to maintain the structure open during composite scaffold fabrication and cell culture. Furthermore, an additional supportive PLGA platform was added by electrospinning to reduce the pore size of the surface and optimize the surface area for cell growth. The resulting 9-ply yarn displayed an average diameter of 34 μm, with a pore length reduction from 900 to 10 μm when PLGA was incorporated into the yarn. Although fibroblast cells attached to the scaffold and remained viable, a clear spatial

heterogeneity and limitations from the use of a glass rod were evidenced.

Other techniques commonly used for the fabrication of 2D structures, such as solvent casting, could also have interest for the preparation of 3D CNT-based scaffolds. Interestingly, Lin et al. demonstrated a faster osteoblast differentiation of mesenchymal stem cells when cultured on PLGA/carboxyl-functionalized MWCNTs films prepared by solvent casting [166]. Recent studies by Rizvi et al. showed 1,4-dioxane as a better solvent than chloroform for the preparation of this type of composites [167]. Meng et al. have also reported the fabrication of novel CNT-based scaffolds by simple adhesion and spreading of tangled, carboxyl-functionalized SWCNTs on PU substrate films [168], with pore sizes in the range of 50–200 nm. In a different approach, interconnected porous

poly(3-hydroxybutyrate) 3D foams were prepared by using a unique combination of solvent casting and particulate leaching [169], with a reported porosity of 85%. The additional incorporation of MWCNTs (2 wt%) into these structures, by dispersion in the initial polymer solution, allowed the acquisition of reinforced mechanical and conductive properties. Simultaneous addition of an antibacterial bioglass led to a multifunctional 3D scaffold with potential use for tissue engineering applications. In other studies, Pan et al. have used a solution evaporation technique for the fabrication of PCL/MWCNT composite scaffolds [170].

Mikos and colleagues used a thermal-crosslinking particulate leaching procedure (using NaCl as a porogen, 75–90 vol%) for the preparation of highly porous scaffolds made of poly(propylene fumarate), propylene fumarate-diacrylate and dodecyl-functionalized, ultra-short SWCNTs (20–80 nm in length) [171]. The resulting structures were prepared as either cylindrical monoliths (4 mm in diameter, 8 mm in height) or circular disk samples (6.5 mm in diameter, 2 mm in thickness). All of them showed porosity percentages from 73 to 91% and pore interconnectivity across, at least, 20 μm and up to 200 μm. Pore size ranged from 40–50 μm (scaffolds with 75 vol% of NaCl) to 80–100 μm (80, 85 and 90 vol% of NaCl). Additional studies demonstrated adhesion and proliferation of marrow stromal cells on these scaffolds. Further work by these authors revealed favorable hard and soft tissue responses when similar scaffolds were implanted in femoral condyles and subcutaneous pockets in rabbits [172]. Specifically, a 3-fold bone tissue ingrowth, reduced inflammatory cell density and increased connective tissue organization were observed at 12 weeks. In a different approach, a phase-separation procedure was reported for the preparation of SWCNT/PLLA scaffolds, with pores of about 100 μm in diameter and suitability for bone regeneration [173]. Those matrices containing 0.5 wt% of CNTs showed the highest enhancement of proliferation and osteoblast differentiation of bone marrow-derived stroma cells when tested *in vitro*. A spark plasma sintering method has been also described for the preparation of polycarbosilane/MWCNT composites with potential use as bone substitutes and dental implants [30].

4. Unraveling CNT toxicity

Despite the evident benefits of using polymers as dispersant and agglutinant agents on the fabrication of 3D CNT-based scaffolds, one must still concern about what happens after polymer-based scaffolds are degraded and CNTs get then in direct contact with cells and tissues inside the body. In order to answer this question, we hereby discuss relevant works on the toxicity of CNTs in dispersion, as it will be ultimately the non-biodegradable material that biological systems will be exposed to and need to get rid of without inducing further cell or tissue damage. Specifically, we center on the role played by size and surface functionalization, as major responsible parameters for toxic responses induced by CNT rigidity and aggregation. Finally,

the biodistribution of CNTs once in the blood stream and their posterior renal excretion is also presented.

4.1. Asbestos-like behavior of CNTs

CNT size, defined by both length and diameter, has been postulated as one of the CNT properties that most decisively influences their toxicity [174], leading to their comparison with asbestos for those long and rigid [175–177]. In this sense, outstanding studies by Donaldson and colleagues compared the toxicity of four types of MWCNTs with different lengths (*i.e.*, from 1 to 56 μm) after intraperitoneal injection (50 μg) in mice and their potential ability to induce mesotheliomas [178]. Results from this work revealed a length-dependent pathogenic effect on the abdominal mesothelial lining for those non-functionalized MWCNTs of length higher than 10 μm, with proven inflammation at 1 day and formation of granulomas after 7 days. The study of the long-term progression of these granulomas remained as a challenge. These toxic effects were associated to a frustrated phagocytosis mediated by fiber-type materials (Fig. 8). Particularly, toxicologists have described fibers as hazardous materials when displaying diameters lower than 3 μm and lengths higher than 20 μm, but also if they remain persistent in the lung tissues without dissolving or breaking [179]. In addition, fibers can cause chronic inflammation, genotoxicity, fibrosis, and cancer if administered and retained in a sufficiently high dose [180]. According to previous results by others [83,181], CNT diameter could have also played a decisive role in the tissue response observed, as those CNTs inducing significant granulomas were the longest but also the widest ones (85 and 165 nm in diameter), when compared to tangled MWCNTs that did not induce either inflammation or granuloma formation (10 and 15 nm in diameter, 1–20 μm in length). Moreover, the fact that the tangled MWCNTs used were carboxyl-functionalized might have also decisively mitigated their toxicity, since functionalization has been proven to reduce CNT toxicity as will be later discussed. Similar studies by Moussa and colleagues indicated 10 μm as the critical length to start inducing granuloma formation, although CNTs with sizes around 5 μm were retained inside the cells for over 5 months [182]. According to this length limitation, Muller et al. recently reported on the absence of carcinogenic responses (mesothelioma, peritoneal tumors and others) two years after administration of non-functionalized MWCNTs (11.3 nm in diameter, 0.7 μm in length) in the peritoneal cavity of rats [183], even when previously demonstrated to induce pulmonary inflammation and granuloma formation [175]. These authors attributed these controversial findings to the reduced number of MWCNTs with a length superior to 5 μm, prompted to promote tumor responses in this animal model [184], and to their ability to quench radical species.

Reports by Nagai et al. associated the deleterious effects of non-functionalized MWCNTs on human MeT5A mesothelial cells with their diameter-dependent piercing of cell membranes, *in vivo* inflammogenicity and formation of mesotheliomas (Fig. 9) [181]. Particularly, thin MWCNTs with a diameter around 50 nm and high crystallinity (*e.g.*,

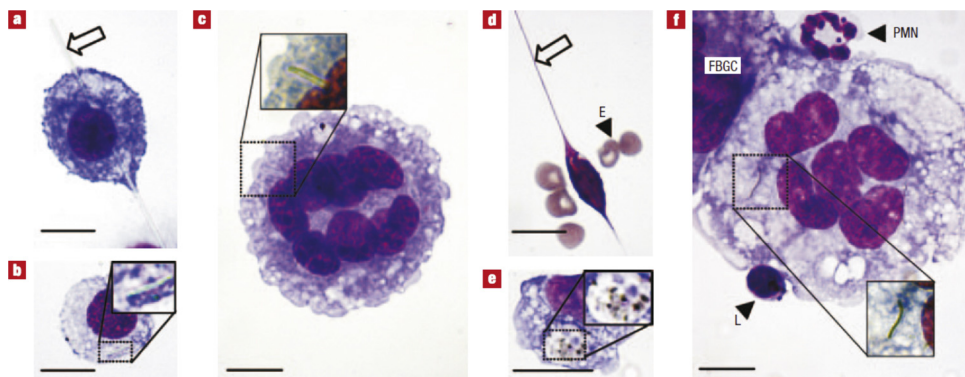


Fig. 8. Images illustrating frustrated phagocytosis by peritoneal macrophages after exposure to short-fiber amosite (SFA), long-fiber amosite (LFA) and different types of MWCNTs (NT_{long2} and NT_{tang1}). Histological sections show the failed incorporation of LFA (a) and NT_{long2} (d). They also indicate the successful phagocytosis of SFA (b) and NT_{tang1} (e). Representative image of a foreign body giant cell (FBGC) after injection of LFA containing short fragments of fibers (c). FBGC is also present after injection of NT_{long2} (f). All images are shown at $1000\times$ magnification and scale bars represent 5 μm . For more details, please refer to the citation. [178], Copyright 2008, Reproduced with permission from the Nature Publishing Group.

high sharpness and rigidity) showed the highest malignancy. On the contrary, MWCNTs either thicker (ca. 150 nm in diameter) or tangled (2–20 nm in diameter) resulted less toxic and carcinogenic. In all cases, CNT length was typically under 10 μm . Kanno and colleagues also published on the asbestos-like toxicity of CNTs when administered

intraperitoneally [185]. Similarly, recent reports by Kane and co-workers described the use of a non-adherent macrophage 3D culture on agarose to compare the toxicity of three commercially available and non-functionalized MWCNTs with asbestos [186]. Results from this work evidenced formation of stable granuloma-like aggregates.

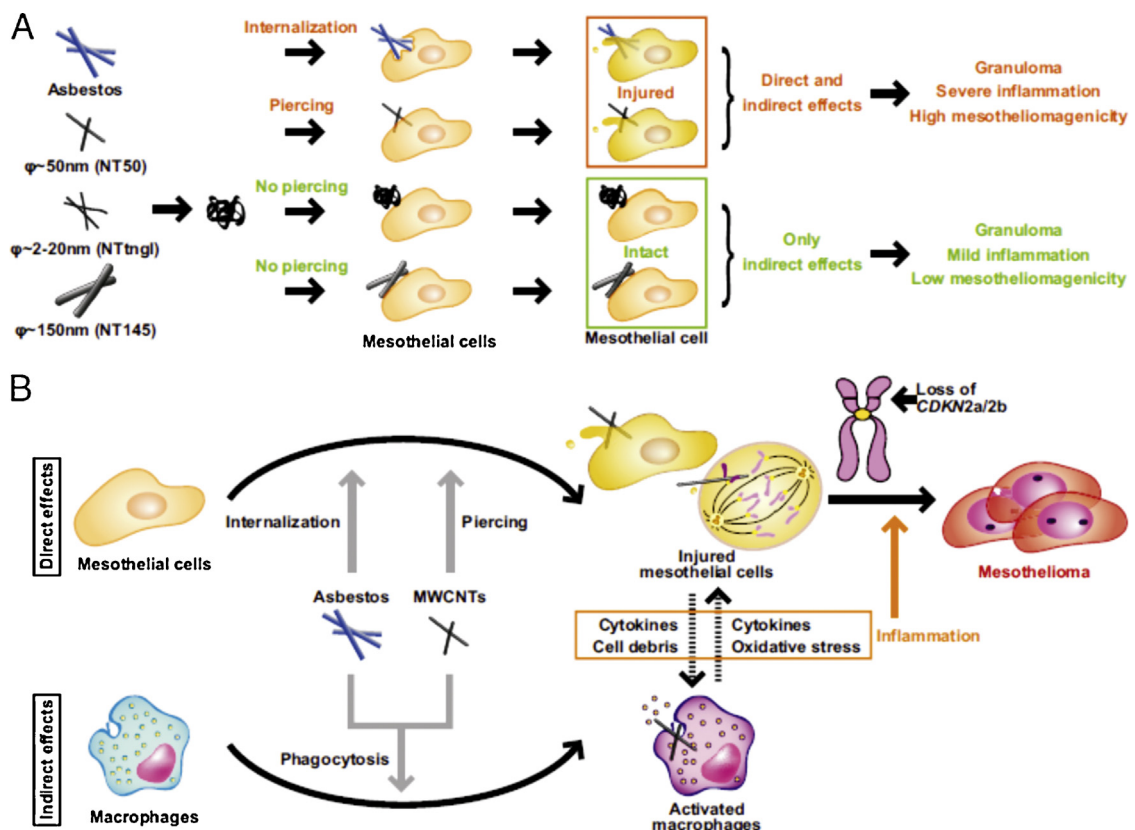


Fig. 9. Scheme of MWCNT effects on mesothelial cells. (A) Asbestos and thin, rigid MWCNTs (50 nm in diameter) penetrate mesothelial cells, thus inducing cell damage. However, MWCNT aggregates (2–20 nm in diameter) and thick MWCNTs (150 nm in diameter) do not penetrate mesothelial cells and therefore do not produce cell damage. (B) Scheme for mechanisms of mesotheliomagenesis in relation to asbestos and MWCNTs [181], Copyright 2011, Reproduced with permission from PNAS.

Table 2

Major physicochemical CNT parameters leading to controversial toxicity in biological systems.

Type	Model	Toxic dose	Diameter (nm)	Length (μm)	Rigidity	Functionalization	Agglomeration	Reference
SWCNT	<i>In vitro</i>	7.5 μg mL ⁻¹	0.5–2	<1 10–20	No	Yes	Aggregates Bundles	[189]
SWCNT	<i>In vitro</i>	12.5 μg mL ⁻¹	2	0.5	No	Yes	No	[208]
MWCNT	<i>In vitro</i>	25 μg mL ⁻¹	50	5	Yes	Yes	No	[208]
MWCNT	<i>In vivo</i>	Non toxic (100 μg mL ⁻¹)	10–15	1–20	No	Yes	Agglomerates	[178]
MWCNT	<i>In vivo</i>	50 μg per mouse 100 μg mL ⁻¹	85–165	> 10	Yes	No	Bundles/ropes	[178]
MWCNT	<i>In vitro</i>	Non toxic (500 μg mL ⁻¹)	15	3	No	No	Yes (tangled)	[181]
MWCNT	<i>In vitro</i>	500 μg mL ⁻¹ (= 5 μg cm ⁻²)	50	5	Yes	No	Yes	[181]
MWCNT	<i>In vitro</i>	1 mg mL ⁻¹						
MWCNT	<i>In vitro</i>	500 μg mL ⁻¹ (= 5 μg cm ⁻²)	115	5	Yes	No	No	[181]
MWCNT	<i>In vivo</i>	10 mg mL ⁻¹						
MWCNT	<i>In vitro</i>	Non toxic (500 μg mL ⁻¹) 10 mg mL ⁻¹	145	4	Yes	No	No	[181]
MWCNT	<i>In vivo</i>	0.5 μg mL ⁻¹ (= 0.38 μg cm ⁻²)	35 85 140	30 13 7	Yes	No	No	[186]
MWCNT	<i>In vitro</i>	0.02 μg mL ⁻¹	20	–	No	Yes/no	–	[82]
MWCNT	<i>In vitro</i>	40 μg mL ⁻¹	20–40	1–5	No	Yes/no	No	[207]

At 7–14 days, macrophages exposed to both asbestos and MWCNTs co-expressed pro-inflammatory and pro-fibrotic phenotypic markers. These authors correlated the induction of epithelioid granulomas with high aspect ratios, rather than the presence of metal residues or high surface area. In conclusion, strong evidence support fiber-type toxicity similar to asbestos for those CNTs with both lengths and diameters high enough, in comparison to cell size, to make them behave as rigid fibers that pierce cell membranes (Table 2).

4.2. Surface functionalization as a tool to mitigate CNT toxicity

Since pristine CNTs tend to agglomerate because of their intrinsic hydrophobic nature, it is difficult to obtain a homogeneous dispersion of CNTs in most of solvents [187]. This aggregation tendency has been identified as another major responsible factor for the cytotoxic effects described for CNTs [188–191], along with CNT surface chemistry and reactivity [192]. For instance, SWCNT agglomerates of submicron sizes were found more toxic than similar concentrations of SWCNTs as bundles (10–20 parallel aligned tubes) [189]. In this context, CNT functionalization has demonstrated to satisfactorily circumvent this important limitation [1], further permitting the immobilization of bioactive molecules on the CNT backbone and avoiding the use of surfactants that often associate with cell toxicity problems [193,194]. Different strategies for the modification of CNTs have been explored, being oxidation with strong acids (e.g., nitric and sulfuric acids) the most extensively used [195]. This acidic treatment allows additional CNT purification, as it removes any metal catalyst residues and carbonaceous deposits, while creating carboxylic acid groups at the ends and side-walls of

the CNTs (carboxyl functionalization). These newly formed functional groups increase CNT solubility, by reducing van der Waals interactions between tubes, and allow further functionalization upon grafting of organic moieties by amide and ester bond formation (organic moiety functionalization) [196] that could favor a more biocompatible interface with cells. Moreover, the chemical nature of the functionalization seems to affect CNT stability in biological media. For instance, Kane and co-workers observed a lower biodurability (only 90 days) for carboxylated SWCNTs in comparison to ozone-treated and aryl-sulfonated ones after incubation in a phagolysosomal simulating fluid *in vitro* [197]. Ozone treatments have been also used by others for rapid MWCNT functionalization [198], with improved cell adhesion and proliferation responses on vertically aligned MWCNT films [199,200]. Finally, numerous hydrophilic organic molecules have been coupled at the CNT surface for their functionalization, including amino-acids [201], arginine-glycine-aspartic acid-serine (RGDS) cell adhesion sequences [202], biomimetic mucin-like polymers [203], glucosamine [204], poly(ethylene glycol) (PEG) [205], heparin [206], and other human plasma proteins [153].

Despite this success, controversy still exists since some reports have shown higher cytotoxicity for functionalized CNTs (both SWCNTs and MWCNTs) when compared to either pristine ones or other carbon nanomaterials [207,208], as well as good cytocompatibility responses in the absence of any functionalization [72]. For instance, Magrez et al. reported concentration-dependent toxic effects of carboxyl-functionalized MWCNTs (20 nm in diameter, 0.002–0.2 μg mL⁻¹) on the proliferation and viability of three different human lung tumor cell lines (i.e., H596, H446 and Calu-1) [82]. In any case, MWCNTs showed higher cytocompatibility than both CNFs and carbon black

at the same dose. Unfortunately, findings from this work might have been affected by the limitations of using the MTT assay and the fact that CNTs were administered embedded in a gelatin matrix. Additionally, it is hard to estimate the significance of the differences between pristine and functionalized MWCNTs as no statistical analysis was performed. Studies by Bottini et al. also revealed higher toxicity for carboxyl-functionalized MWCNTs (20–40 nm in diameter, 1–5 μm in length) than for pristine ones when in contact with Jurkat lymphocytes, but only at concentrations as high as 400 μg mL⁻¹ [207], with a 10-fold lower concentration of either type not being nearly as toxic. In fact, CNT concentration seemed more critical than functionalization in these studies. In a different approach, Tian et al. found carboxyl-functionalized SWCNTs (2 nm in diameter, 500 nm in length) as a more toxic nanomaterial than either MWCNTs (50 nm in diameter, 5 μm in length), active carbon, graphite or carbon black [208]. These authors indicated surface area as a first-order variable responsible for these toxic responses, followed by surface chemistry modulated by functionalization. Contrary to other works, SWCNTs and MWCNTs as bundles were found less harmful than dispersed CNTs obtained after acid treatment. Overall, although the effects of functionalization on CNT toxicity seem to vary significantly among studies, more conclusive evidences exist supporting a beneficial role for this modification than the contrary (Table 2).

4.3. CNT biodistribution from the blood stream and posterior excretion

The non-biodegradability of CNTs will eventually lead to their presence in blood in order to get eliminated. In this sense, Prato and co-workers have published on the tissue biodistribution and half-life in blood of radiolabelled SWCNTs [209]. In further studies, these authors reported on the early tissue response (first 24 h) induced by intravenous administration of non-functionalized, purified and functionalized MWCNTs [210]. Specifically, the degree of CNT functionalization, rather than the nature of the functional groups incorporated, was identified as a more critical factor leading to less tissue accumulation. In additional studies, the authors intended to elucidate critical CNT parameters for urinary excretion [211,212]. Particularly, radiolabelled MWCNTs reached the kidneys and bladder within 1 min after intravenous injection. After 24 h, the majority of MWCNTs were found in the urine. Therefore, water-soluble MWCNTs functionalized by amino-acid conjugation remained in the blood stream a short period of time (*ca.* 24 h) and were mainly excreted by the urinary system. This renal elimination likely occurred through the glomerular filtration system as CNT diameter (e.g., 20–30 nm) was in the range of podocytes (40 nm) and vascular fenestra (30 nm) pores. Furthermore, CNT length (0.5–2 μm) allowed them to pass through the glomerular basal membrane (200–400 nm) [188]. In this sense, it is worth noting that individualized SWCNTs with lengths under 300 nm can escape the reticulo-endothelial system and be excreted through the kidneys and the bile ducts [47]. When tissue accumulation was analyzed in mice, non-functionalized MWCNTs were observed in lung and liver

tissue during the first 24 h post-injection (200 μg injected in serum), along with behavioral and breathing abnormalities. MWCNTs functionalized with ammonium groups were also investigated, with results indicating a clear correlation between tissue accumulation and the degree of functionalization. Specifically, MWCNTs more functionalized with NH₃⁺ groups (0.9 mmol g⁻¹) were absent from any tissue after 24 h; whereas those less functionalized (0.2 mmol g⁻¹) were observed in liver and spleen. Mice treated with MWCNTs functionalized with negative charges behaved similarly. These authors concluded that CNT excretion and tissue accumulation was significantly affected by the degree of functionalization and the ability of CNTs to stay individualized. According to this, studies in mice by Yang et al. reported a major tissue accumulation of pristine SWCNTs in lung, liver and spleen over 28 days [213]. Works by Schipper et al. further confirmed the absence of both acute and chronic toxicity when covalently and non-covalently PEG-functionalized SWCNTs (previously oxidized by nitric acid treatment) were intravenously administered in mice [214]. Neither body weight nor blood parameters were altered during the 4 months of the study. Furthermore, histological studies revealed no apparent tissue toxicity even when SWCNTs were present in liver and spleen macrophages for 4 months. The major limitation of this work was the reduced sample size (*n*=4 per group).

Along these lines, Dai and colleagues studied the distribution and excretion of SWCNTs after intravenous administration in mice for a period of 3 months [192]. SWCNTs non-covalently functionalized with PEGylated phospholipids were injected and detected in the blood stream for up to 1 day, with almost complete clearance from the main organs in 2 months. Low uptake by the reticulo-endothelial system was also confirmed. By using Raman spectroscopy, SWCNTs were identified in the kidney, bladder, intestine, and feces, thus suggesting renal and biliary excretion, respectively. Histological studies did not reveal apparent toxic effects in blood or tissues, according to previous results by others, although a major accumulation in liver and spleen was evidenced as early as 1 day. The authors outlined the utility of Raman spectroscopy to detect CNTs in blood and their biodistribution in tissues and organs without common labeling limitations such as photo-bleaching over time. Isotope ratio mass spectroscopy, coupled with ¹³C-enriched samples, has been reported as well as an effective technique for biodistribution studies of nanomaterials [213]. Similarly, magnetic resonance imaging has been applied to monitor gadolinium-labeled SWCNTs released from PLGA scaffolds [215]. More recent studies have proposed multiscale photoacoustic microscopy as a non-invasive useful technique to monitor and characterize SWCNTs embedded into biodegradable substrates [216].

5. Final discussion and conclusions

This review intended to outline the promising role that polymers play on the design of more biocompatible 3D CNT-based scaffolds for biomedical applications. To this attempt, we have first exposed efforts on the fabrication of bare CNT-based 3D substrates and their major

Table 3

Physicochemical characteristics of CNTs strongly related to their toxicity in biological systems.

Type	Model	Dose ($\mu\text{g mL}^{-1}$)	Diameter	Length	Rigidity	Functionalization	Agglomeration	Toxic effects	Exemplary references
SWCNT	<i>In vitro</i>	7.5	Narrower	Longer	No	Yes	Yes	Yes	[189]
SWCNT	<i>In vitro</i>	100	7.5	Narrower	Shorter	No	Yes	Yes	[189]
MWCNT	<i>In vivo</i>	100	Wider	Longer	Yes	No	Yes	Yes	[178]
MWCNT	<i>In vitro</i>	0.5	Wider	Shorter	Yes	No	No	Yes	[186]
MWCNT	<i>In vivo</i>	10,000	Wider	Shorter	Yes	No	No	Yes	[181]
MWCNT	<i>In vitro</i>	25	Wider	Shorter	Yes	Yes	No	Yes	[208]
MWCNT	<i>In vivo</i>	1000	Wider	Shorter	No	No	Yes	Yes	[181]
MWCNT	<i>In vitro</i>	0.02	Narrower	–	No	No/yes	–	Yes	[82]
MWCNT	<i>In vivo</i>	100	Narrower	Longer	No	Yes	Yes	No	[178]
MWCNT	<i>In vitro</i>	40	Narrower	Shorter	No	No/yes	No	Yes	[207]

limitations (*i.e.*, structural restrictions and CNT toxicity). These both constraints could be bypassed by using biocompatible polymers for scaffold fabrication. Regarding the first, composites containing functionalized CNTs show better mechanical performance as a result of improved CNT dispersion and stress-strain transfer between CNTs and the polymer matrix by refining their interfacial bonding properties [15]. In this review, we have also revised the most outstanding biocompatible methodologies for the fabrication of 3D CNT-based scaffolds. However, and despite the extensive progress to this respect, most of these approaches result in structurally patterned 2D substrates or 3D scaffolds with either a very limited third dimension or inadequate porosity for cell colonization, frequently not even interconnected in a useful fashion for homogeneous distribution of cells. For instance, matrices obtained by electrospinning or gel formation generally fail on producing homogeneous and reproducible structures in terms of porosity, with pore sizes too small for cell infiltration. In other techniques such as solvent evaporation or LbL deposition, it is not trivial to incorporate any porosity. On the contrary, strategies based on unidirectional freeze-casting and coating of pre-formed 3D structures may provide scaffolds with an ordered architecture and pores ranging in a more suitable size. Unfortunately, the former one likely requires flow-through seeding techniques to guarantee cell migration on the third dimension, while the last one only permits the incorporation of a smaller amount of CNTs, thus reducing the benefits from their attractive properties. Therefore, the preparation of real 3D scaffolds more effectively resembling 3D native tissues still remains a clear challenge for researchers in materials science [49]. In this context, promising emerging technologies such as bioprinting [217], robocasting [218] and solid free-form methodologies, rarely used in the fabrication of CNT-based substrates, may open new avenues to accomplish this aim. Nonetheless, further advances in 3D scaffold preparation will be only possible if assisted by parallel improvements in cell seeding methods, protocols for culture media replacement and analytic methods for cellular behavior in 3D structures, among others [49].

In the context of designing 3D scaffolds, it is worth to mention the relevant role that the own three-dimensionality of the substrate may exert on cell responses. For instance, works by Behan et al. demonstrated superior performance of Schwann cells on 3D,

rather than 2D, CNT-based substrates [156]. In a different approach, enhanced performance of mouse embryonic stem cells was found on matrices based on PET compared to control 2D surfaces [163]. Similar findings have been evidenced on 3D scaffolds without CNTs, including enhanced neural differentiation of mouse embryoid bodies [219], feasible hepatocyte-like differentiation of human embryonic stem cells [220], faster osteogenic differentiation of mouse embryonic fibroblasts [221], and modulation of signaling cascades in breast cancer cells [222]. Even molecular mechanisms governing cell migration differ on 3D matrices and are not mimicked by those on 2D [223]. Taken together, these results encourage further efforts on the preparation of 3D scaffolds as more advanced and smart platforms for the repair and/or substitution of damaged and diseased human tissues. In this sense, the use of CNTs in combination with biocompatible polymers might offer additional attractive properties, as comprehensively exposed herein.

Finally, careful inspection of relevant works regarding CNT toxicity has evidenced a key role for dose, as expected for any foreign material. Table 3 intends to offer some useful guidelines on the toxic range of concentrations for CNTs. Particularly, amounts in the order of a few μg (typically below 100 μg) bring opportunity to avoid toxic responses by CNT modification. Therefore, toxicity seems not to be an inherent property of CNTs, but a circumstantial feature depending on dose and able to be tuned by modulating their physicochemical properties and way of administration. Put in words of Paracelso, “*Dosis sola facit venenum*”. Additionally, the development of decision supporting tools may help researchers to discriminate more efficiently the environmental and health risk of novel nanomaterials, as well as their cost–benefit ratio [224]. In this sense, as extensively discussed in this review, the use of polymers offers an attractive tool to benefit the biocompatibility of CNTs, also permitting approaches at a lower cost as polymer-based strategies are usually more economical than other types of chemical procedures. Fig. 10 shows an example of a preliminary decision tree for the hazard characterization of nanomaterials that could be applied to CNTs.

In conclusion, we strongly believe that strategies comprising the use of biocompatible polymers in the shape of 3D scaffolds containing hydrophilic CNTs within a size range able to be excreted through the urinary system and without fiber type-induced toxicity may significantly

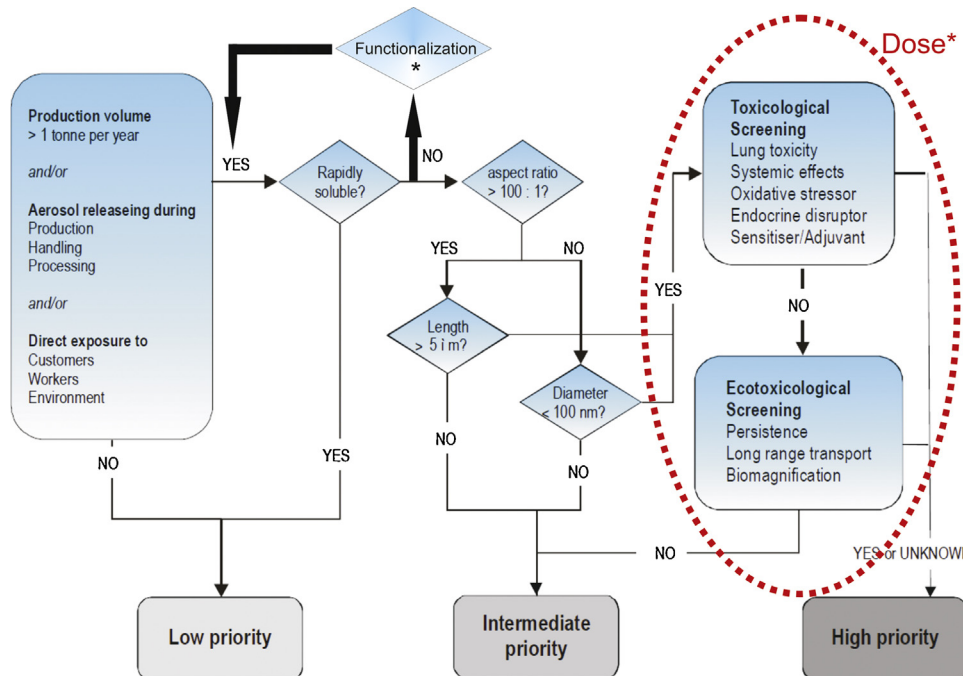


Fig. 10. Exemplary decision tree useful for the hazard characterization of CNT-based materials. Chemical functionalization provides a valuable tool for reducing CNT insolubility in aqueous solutions. Dose should be also critically considered when evaluating CNT toxicity in biological systems. Modifications on the original scheme are marked with asterisks (*) [24]. Copyright 2012, Adapted with permission from the American Chemical Society.

serve for tissue regeneration, as illustrated by promising advances exposed herein. When using these CNT-based materials, results from *in vitro* and *in vivo* studies must be always contextualized, never dramatized or underestimated, to avoid false expectations or impair the development of potentially useful novel technologies. We expect this critic review to help research community working on CNTs, and other carbon nanomaterials such as graphene [2], to identify useful guidelines that help advancing their use in biomedical applications.

Acknowledgements

This work has been supported by MINECO (grant reference numbers MAT2009-10214, MAT2011-25329 and MAT2012-34811). M.C.S. acknowledges MINECO for a *Juan de la Cierva* fellowship.

Appendix A. Notes

Search results included in Fig. 1 have been obtained from <http://www.scopus.com>. Document type: article or review. Searches included:

TITLE-ABS-KEY ("carbon nanotubes"),
 TITLE-ABS-KEY("carbon nanotubes") AND ALL("polymer"),
 TITLE-ABS-KEY("carbon nanotubes") AND ALL("biomedical applications"),
 TITLE-ABS-KEY("carbon nanotubes") AND ALL("scaffold"),
 TITLE-ABS-KEY("carbon nanotubes") AND ALL("scaffold") AND ALL("biomedical applications"),

TITLE-ABS-KEY("carbon nanotubes") AND ALL("scaffold") AND ALL("polymer"),
 TITLE-ABS-KEY("carbon nanotubes") AND ALL("scaffold") AND ALL("tissue engineering"),
 TITLE-ABS-KEY("carbon nanotubes") AND ALL("scaffold") AND ALL("bone regeneration"), and
 TITLE-ABS-KEY("carbon nanotubes") AND ALL("scaffold") AND ALL("nerve regeneration"). Last retrieved: 11/25/2013.

References

- [1] Tran PA, Zhang L, Webster TJ. Carbon nanofibers and carbon nanotubes in regenerative medicine. *Adv Drug Deliv Rev* 2009;61:1097–114.
- [2] Bussy C, Ali-Boucetta H, Kostarelos K. Safety considerations for graphene: lessons learnt from carbon nanotubes. *Acc Chem Res* 2013;46:692–701.
- [3] Graham AP, Duesberg GS, Seidel RV, Liebau M, Unger E, Pamler W, Kreupl F, Hoenlein W. Carbon nanotubes for microelectronics. *Small* 2005;1:382–90.
- [4] Dai H. Carbon nanotubes: synthesis integration and properties. *Acc Chem Res* 2002;35:1035–44.
- [5] Journet C, Maser WK, Bernier P, Loiseau A, Lamy de la Chapelle M, Lefrant S, Deniard P, Lee R, Fischer JE. Large-scale production of single-walled carbon nanotubes by the electric-arc technique. *Nature* 1997;388:756–8.
- [6] Thess A, Lee R, Nikolaev P, Dai HJ, Petit P, Robert J, Xu C, Lee YH, Kim SG, Rinzler AG, Colbert DT, Scuseria GE, Tománek D, Fischer JE, Smalley RE. Crystalline ropes of metallic carbon nanotubes. *Science* 1996;273:483–7.
- [7] Cassell AM, Raymakers JA, Kong J, Dai HJ. Large scale CVD synthesis of single-walled carbon nanotubes. *J Phys Chem B* 1999;103:6484–92.
- [8] Correa-Duarte MA, Wagner N, Rojas-Chapana J, Morszeck C, Thie M, Giersig M. Fabrication and biocompatibility of carbon nanotube-based 3D networks as scaffolds for cell seeding and growth. *Nano Lett* 2004;4:2233–6.

- [9] Treacy MMJ, Ebbesen TW, Gibson JM. Exceptionally high Young's modulus observed for individual carbon nanotubes. *Nature* 1996;381:678–80.
- [10] Yu MF, Lourie O, Dyer MJ, Moloni K, Kelly TF, Ruoff RS. Strength and breaking mechanism of multiwalled carbon nanotubes under tensile load. *Science* 2000;287:637–40.
- [11] Thostenson ET, Ren Z, Chou TW. Advances in the science and technology of carbon nanotubes and their composites: a review. *Compos Sci Technol* 2001;61:1899–912.
- [12] Bradford P, Bogdanovich A. Electrical conductivity study of carbon nanotube yarns 3-D hybrid braids and their composites. *J Compos Mater* 2008;42:1533–45.
- [13] Oberlin A, Endo M, Koyama T. Filamentous growth of carbon through benzene decomposition. *J Cryst Growth* 1976;32:335–49.
- [14] Iijima S. Helical microtubules of graphitic carbon. *Nature* 1991;354:56–8.
- [15] Byrne MT, Gun'ko YK. Recent advances in research on carbon nanotube–polymer composites. *Adv Mater* 2010;22:1672–88.
- [16] Coleman JN, Khan U, Gun'ko YK. Mechanical reinforcement of polymers using carbon nanotubes. *Adv Mater* 2006;18:689–706.
- [17] Chen RJ, Bangsaruntip S, Drouvalakis KA, Kam NWS, Shim M, Li Y, Kim W, Utz PJ, Dai H. Noncovalent functionalization of carbon nanotubes for highly specific electronic biosensors. *Proc Natl Acad Sci U S A* 2003;100:4984–9.
- [18] Besteman K, Lee JO, Wiertz FGM, Heering HA, Dekker C. Enzyme-coated carbon nanotubes as single-molecule biosensors. *Nano Lett* 2003;3:727–30.
- [19] Wang J, Musameh M, Lin YH. Solubilization of carbon nanotubes by NaOH toward the preparation of amperometric biosensors. *J Am Chem Soc* 2003;125:2408–9.
- [20] Minoux E, Groening O, Teo KK, Dalal SH, Gangloff L, Schnell JP, Hudanski L, Bu IYY, Vincent P, Legagneux P, Amarantunga GAJ, Milne WI. Achieving high-current carbon nanotube emitters. *Nano Lett* 2005;5:2135–8.
- [21] Patchkovskii S, Tse JS, Yurchenko SN, Zhechkov L, Heine T, Seifert G. Graphene nanostructures as tunable storage media for molecular hydrogen. *Proc Natl Acad Sci U S A* 2005;102:10439–44.
- [22] Wilson NR, Macpherson JV. Carbon nanotube tips for atomic force microscopy. *Nat Nanotechnol* 2009;4:483–91.
- [23] Vakarelski IU, Brown SC, Higashitani K, Moudgil BM. Penetration of living cell membranes with fortified carbon nanotube tips. *Langmuir* 2007;23:10893–6.
- [24] Ebron VH, Yang Z, Seyer DJ, Kozlov ME, Oh J, Xie H, Razal J, Hall LJ, Ferraris JP, MacDiarmid AG, Baughman RH. Fuel-powered artificial muscles. *Science* 2006;311:1580–3.
- [25] Veetil JV, Ye K. Tailored carbon nanotubes for tissue engineering applications. *Biotechnol Prog* 2009;25:709–21.
- [26] Harrison BS, Atala A. Carbon nanotube applications for tissue engineering. *Biomaterials* 2007;28:344–53.
- [27] Bianco A, Kostarelos K, Partidos CD, Prato M. Biomedical applications of functionalized carbon nanotubes. *Chem Commun* 2005;5:571–7.
- [28] Nayak TR, Jian L, Phua LC, Ho HK, Ren Y, Pastorin G. Thin films of functionalized multiwalled carbon nanotubes as suitable scaffold materials for stem cells proliferation and bone formation. *ACS Nano* 2010;4:7717–25.
- [29] Jell G, Verdejo R, Safinia L, Shaffer MSP, Stevens MM, Bismarck A. Carbon nanotube-enhanced polyurethane scaffolds fabricated by thermally induced phase separation. *J Mater Chem* 2008;18:1865–72.
- [30] Wang W, Watari F, Omori M, Liao S, Zhu Y, Yokoyama A, Uo M, Kimura H, Ohkubo A. Mechanical properties and biological behavior of carbon nanotube/polycarbosilane composites for implant materials. *J Biomed Mater Res B* 2007;82:223–30.
- [31] Zanello LP, Zhao B, Hu H, Haddon RC. Bone cell proliferation on carbon nanotubes. *Nano Lett* 2006;6:562–7.
- [32] Lovat V, Pantarotto D, Lagostena L, Cacciari B, Grandolfo M, Righi M, Spalluto G, Prato M, Ballerini L. Carbon nanotube substrates boost neuronal electrical signaling. *Nano Lett* 2005;5:1107–10.
- [33] Jan E, Kotov NA. Successful differentiation of mouse neural stem cells on layer-by-layer assembled single-walled carbon nanotube composite. *Nano Lett* 2007;7:1123–8.
- [34] Gheith MK, Sinani VA, Wicksted JP, Matts RL, Kotov NA. Single-walled carbon nanotube polyelectrolyte multilayers and freestanding films as a biocompatible platform for neuroprosthetic implants. *Adv Mater* 2005;17:2663–70.
- [35] Wei W, Sethuraman A, Jin C, Monteiro-Riviere NA, Narayan RJ. Biological properties of carbon nanotubes. *J Nanosci Nanotechnol* 2007;7:1284–97.
- [36] Hu H, Ni Y, Mandal SK, Montana V, Zhao B, Haddon RC, Parpura V. Polyethylenimine functionalized single-walled carbon nanotubes as a substrate for neuronal growth. *J Phys Chem B* 2005;109:4285–9.
- [37] Meng J, Kong H, Xu HY, Song L, Wang CY, Xie SS. Improving the blood compatibility of polyurethane using carbon nanotubes as fillers and its implications to cardiovascular surgery. *J Biomed Mater Res A* 2005;74:208–14.
- [38] Endo M, Koyama S, Matsuda Y, Hayashi T, Kim YA. Thrombogenicity and blood coagulation of a microcatheter prepared from carbon nanotube–nylon-based composite. *Nano Lett* 2005;5:101–5.
- [39] Kam NWS, O'Connell M, Wisdom JA, Dai H. Carbon nanotubes as multifunctional biological transporters and near-infrared agents for selective cancer cell destruction. *Proc Natl Acad Sci U S A* 2005;102:11600–5.
- [40] Singh R, Pantarotto D, McCarthy D, Chaloin O, Hoebeke J, Partidos CD, Briand JP, Prato M, Bianco A, Kostarelos K. Binding and condensation of plasmid DNA onto functionalized carbon nanotubes: toward the construction of nanotube-based gene delivery vectors. *J Am Chem Soc* 2005;127:4388–96.
- [41] Nepal D, Sohn JL, Aicher WK, Lee S, Geckeler KE. Supramolecular conjugates of carbon nanotubes and DNA by a solid-state reaction. *Biomacromolecules* 2005;6:2919–22.
- [42] Cai D, Matazara JM, Qin ZH, Huang Z, Huang J, Chiles TC, Carnahan D, Kempa K, Ren Z. Highly efficient molecular delivery into mammalian cells using carbon nanotube spearing. *Nat Methods* 2005;2:449–54.
- [43] Venkatesan N, Yoshimitsu J, Ito Y, Shibataand N, Takada K. Liquid filled nanoparticles as a drug delivery tool for protein therapeutics. *Biomaterials* 2005;26:7154–63.
- [44] Zhang X, Meng L, Lu Q, Fei Z, Dyson PJ. Targeted delivery and controlled release of doxorubicin to cancer cells using modified single wall carbon nanotubes. *Biomaterials* 2009;30:6041–7.
- [45] ShiKam NW, Jessop TC, Wender PA, Dai H. Nanotube molecular transporters: internalization of carbon nanotube–protein conjugates into mammalian cells. *J Am Chem Soc* 2004;126:650–1.
- [46] ShiKam NW, Liu Z, Dai H. Functionalization of carbon nanotubes via cleavable disulfide bonds for efficient intracellular delivery of siRNA and potent gene silencing. *J Am Chem Soc* 2005;127:12492–3.
- [47] Cui HF, Vashist SK, Al-Rubeann K, Luong JHT, Sheu FS. Interfacing carbon nanotubes with living mammalian cells and cytotoxicity issues. *Chem Rev Toxicol* 2010;23:1131–47.
- [48] Dvir T, Timko BP, Kohane DS, Langer R. Nanotechnological strategies for engineering complex tissues. *Nat Nanotechnol* 2011;6:13–22.
- [49] Lee J, Cuddihy M, Kotov NA. Three-dimensional cell culture matrices: state of the art. *Tissue Eng Part B Rev* 2008;14:61–86.
- [50] Rutkowski GE. Engineered tissue. In: Webster JG, editor. Encyclopedia of medical devices and instrumentation. 2nd ed Hoboken: John Wiley & Sons, Inc; 2006, p. 3022.
- [51] Shanbhag S, Wang S, Kotov NA. Cell distribution profiles in three-dimensional scaffolds with inverted-colloidal-crystal geometry: modeling and experimental investigations. *Small* 2005;1:1208–14.
- [52] Nardecchia S, Carriazo D, Ferrer ML, Gutiérrez MC, del Monte F. Three dimensional macroporous architectures and aerogels built of carbon nanotubes and/or graphene: synthesis and applications. *Chem Soc Rev* 2013;42:794–830.
- [53] Martin CR, Kohli P. The emerging field of nanotube biotechnology. *Nat Rev Drug Discov* 2003;2:29–37.
- [54] Saito N, Aoki K, Usui Y, Shimizu M, Hara K, Narita N, Ogihara N, Nakamura K, Ishigaki N, Kato H, Hanju H, Taruta S, Ahm K, Endo M. Application of carbon fibers to biomaterials: a new era of nano-level control of carbon fibers after 30-years of development. *Chem Soc Rev* 2011;40:3824–34.
- [55] Fisher C, Rider AE, Jun-Han Z, Kumar S, Levchenko I, Ostrikov K. Applications and nanotoxicity of carbon nanotubes and graphene in biomedicine. *J Nanomater* 2012;315185:1–19.
- [56] Liu Z, Robinson JT, Tabakman SM, Yang K, Dai H. Carbon materials for drug delivery and cancer therapy. *Mater Today* 2011;14:316–23.
- [57] Yang K, Feng L, Shi X, Liu Z. Nano-graphene in biomedicine: therapeutic applications. *Chem Soc Rev* 2013;42:530–47.
- [58] Edwards SL, Werkmeister JA, Ramshaw JAM. Carbon nanotubes in scaffolds for tissue engineering. *Expert Rev Med Devices* 2009;6:499–505.
- [59] Li X, Fan Y, Watari F. Current investigations into carbon nanotubes for biomedical application. *Biomed Mater* 2010;5:22001.

- [60] Haniu H, Saito N, Matsuda Y, Tsukahara T, Usui Y, Narita N, Hara K, Aoki K, Shimizu M, Ogiwara N, Takanashi S, Okamoto M, Kobayashi S, Ishigaki N, Nakamura K, Kato H. Basic potential of carbon nanotubes in tissue engineering applications. *J Nanomater* 2012;1–10, 343747.
- [61] Saito N, Usui Y, Aoki K, Narita N, Shimizu M, Hara K, Ogiwara N, Nakamura K, Ishigaki N, Kato H, Taruta S, Endo M. Carbon nanotubes: biomaterial applications. *Chem Soc Rev* 2009;38: 1897–903.
- [62] Yang ST, Luo J, Zhou Q, Wang H. Pharmacokinetics metabolism and toxicity of carbon nanotubes for bio-medical purposes. *Theranostics* 2012;2:271–82.
- [63] Saito N, Usui Y, Aoki K, Narita N, Shimizu M, Ogiwara N, Nakamura K, Ishigaki N, Kato H, Taruta S. Carbon nanotubes for biomaterials in contact with bone. *Curr Med Chem* 2008;15:523–7.
- [64] Narita N, Kobayashi Y, Nakamura H, Maeda K, Ishihara A, Mizoguchi T, Usui Y, Aoki K, Shimizu M, Kato H, Ozawa H, Udagawa N, Endo M, Takahashi N, Saito N. Multiwalled carbon nanotubes specifically inhibit osteoclast differentiation and function. *Nano Lett* 2009;9:1406–13.
- [65] Shimizu M, Kobayashi Y, Mizoguchi T, Nakamura H, Kawahara I, Narita N, Usui Y, Aoki K, Hara K, Haniu H, Ogiwara N, Ishigaki N, Nakamura K, Kato H, Kawakubo M, Dohi Y, Taruta S, Kim YA, Endo M, Ozawa H, Udagawa N, Takahashi N, Saito N. Carbon nanotubes induce bone calcification by bidirectional interaction with osteoblasts. *Adv Mater* 2012;24:2176–85.
- [66] Pandey G, Thostenson ET. Carbon nanotube-based multifunctional polymer nanocomposites. *Polym Rev* 2012;52:355–416.
- [67] Bounioux C, Katz EA, Yerushalmi-Rosen R. Conjugated polymers – carbon nanotubes-based functional materials for organic photovoltaics: a critical review. *Polym Adv Technol* 2012;23: 1129–40.
- [68] Sahoo NG, Rana S, Cho JW, Li L, Chan SH. Polymer nanocomposites based on functionalized carbon nanotubes. *Prog Polym Sci* 2010;35:837–67.
- [69] Moniruzzaman M, Winey KI. Polymer nanocomposites containing carbon nanotubes. *Macromolecules* 2006;39:5194–205.
- [70] Laird ED, Li CY. Structure and morphology control in crystalline polymer–carbon nanotube nanocomposites. *Macromolecules* 2013;46:2877–91.
- [71] Spitalsky Z, Tasis D, Papagelis K, Galiotis C. Carbon nanotube–polymer composites: chemistry processing mechanical and electrical properties. *Prog Polym Sci* 2010;35:357–401.
- [72] Lobo O, Antunes EF, Palma MB, Pacheco-Soares C, Travá-Airoldi VJ, Corat Ej. Monolayer formation of human osteoblastic cells on vertically aligned multiwalled carbon nanotube scaffolds. *Cell Biol Int* 2010;34:393–8.
- [73] Lobo AO, Corat MAF, Antunes EF, Palma MBS, Pacheco-Soares C, Garcia EE, Corat Ej. An evaluation of cell proliferation and adhesion on vertically-aligned multi-walled carbon nanotube films. *Carbon* 2010;48:245–54.
- [74] Lobo AO, Antunes EF, Machado AHA, Pacheco-Soares C, Travá-Airoldi VJ, Corat Ej. Cell viability and adhesion on as grown multi-wall carbon nanotube films. *Mater Sci Eng C* 2008;28:264–9.
- [75] Liu H, Li S, Zhai J, Li H, Zheng Q, Jiang L, Zhu D. Self-assembly of large-scale micropatterns on aligned carbon nanotube films. *Angew Chem Int Ed Engl* 2004;43:1146–9.
- [76] Sorkin R, Greenbaum A, David-Pur M, Anava S, Ayali A, Ben-Jacob E, Hanein Y. Process entanglement as a neuronal anchorage mechanism to rough surfaces. *Nanotechnology* 2009;20:015101, 1–8.
- [77] Gabay T, Jakobs E, Ben-Jacob E, Hanein Y. Engineered self-organization of neural networks using carbon nanotube clusters. *Physica A* 2005;350:611–21.
- [78] Huang YJ, Wu HC, Tai NH, Wang TW. Carbon nanotube rope with electrical stimulation promotes the differentiation and maturity of neural stem cells. *Small* 2012;8:2869–77.
- [79] Cellot G, Ballerini L, Prato M, Bianco A. Neurons are able to internalize soluble carbon nanotubes: new opportunities or old risks. *Small* 2010;6:2630–3.
- [80] Ding L, Stilwell J, Zhang T, Elboudwarej O, Jiang H, Selegue JP, Cooke PA, Gray JW, Chen FF. Molecular characterization of the cytotoxic mechanism of multiwall carbon nanotubes and nano-onions on human skin fibroblast. *Nano Lett* 2005;5:2448–64.
- [81] Silva VM, Corson N, Elder A, Oberdoerster G. The rat ear vein model for investigation *in vivo* thrombogenicity of ultrafine particles (UFP). *Toxicol Sci* 2005;85:983–9.
- [82] Magrez A, Kasas S, Salicchio V, Pasquier N, Seo JW, Celio M, Catsicas S, Schwaller B, Forró L. Cellular toxicity of carbon-based nanomaterials. *Nano Lett* 2006;6:1121–5.
- [83] Mwenifumbo S, Shaffer MS, Stevens MM. Exploring cellular behaviour with multi-walled carbon nanotube constructs. *J Mater Chem* 2007;17:1894–902.
- [84] Sayes CM, Fortner JD, Guo W, Lyon D, Boyd AM, Ausman KD, Tao YJ, Sitharaman B, Wilson LJ, Hughes JB, West JL, Colvin VL. The differential cytotoxicity of water-soluble fullerenes. *Nano Lett* 2004;4:1881–7.
- [85] van der Zande M, Junker R, Walboomers XF, Jansen JA. Carbon nanotubes in animal models: a systematic review on toxic potential. *Tissue Eng Part B* 2011;17:57–69.
- [86] Liu Y, Zhao Y, Sun B, Chen C. Understanding the toxicity of carbon nanotubes. *Acc Chem Res* 2013;46:702–13.
- [87] Guo L, Von Dem Bussche A, Buechner M, Yan A, Kane AB, Hurt RH. Adsorption of essential micronutrients by carbon nanotubes and the implications for nanotoxicity testing. *Small* 2008;4: 721–7.
- [88] Ge C, Du J, Zhao L, Wang L, Liu Y, Li D, Yang Y, Zhou R, Zhao Y, Chai Z, Chen C. Binding of blood proteins to carbon nanotubes reduces cytotoxicity. *Proc Natl Acad Sci U S A* 2011;108:16968–73.
- [89] Wang SF, Shen L, Zhang WD, Tong YJ. Preparation and mechanical properties of chitosan/carbon nanotubes composites. *Biomacromolecules* 2005;6:3067–72.
- [90] Pow BYF, Mak AFT, Man SW, Yang M. Poly(L-lactide)/multiwalled carbon nanotube composites: interaction with osteoblast-like cells in vitro. *Adv Mat Res* 2008;47–50(Part 2):1347–50.
- [91] Mamedov AA, Kotov NA, Prato M, Guldi DM, Wicksted JP, Hirsch A. Molecular design of strong single-wall carbon nanotube/polyelectrolyte multilayer composites. *Nat Mater* 2002;1:190–4.
- [92] Olivas-Armendáriz I, García-Casillas P, Martínez-Sánchez R, Martínez-Villafáñez A, Martínez-Pérez CA. Chitosan/MWCNT composites prepared by thermal induced phase separation. *J Alloys Compd* 2010;495:592–5.
- [93] Abarrategi A, Gutiérrez MC, Moreno-Vicente C, Hortigüela MJ, Ramos V, López-Lacomba JL, Ferrer ML, del Monte F. Multiwall carbon nanotube scaffolds for tissue engineering purposes. *Biomaterials* 2008;29:94–102.
- [94] Hortigüela MJ, Gutiérrez MC, Aranaz I, Jobbág M, Abarrategi A, Moreno-Vicente C, Civantos A, Ramos V, López-Lacomba JL, Ferrer ML, del Monte F. Urea assisted hydroxyapatite mineralization on MWCNT/CHI scaffolds. *J Mater Chem* 2008;18:5933–40.
- [95] Nardiechia S, Serrano MC, Gutiérrez MC, Portolés MT, Ferrer ML, del Monte F. Osteoconductive performance of carbon nanotube scaffolds homogeneously mineralized by flow-through electrodeposition. *Adv Funct Mater* 2012;22:4411–20.
- [96] Lau C, Cooney MJ, Atanassov P. Conductive macroporous composite chitosan–carbon nanotube scaffolds. *Langmuir* 2008;24:7004–10.
- [97] Meng D, Ioannou J, Boccaccini AR. Bioglass®-based scaffolds with carbon nanotube coating for bone tissue engineering. *J Mater Sci Mater Med* 2009;20:2139–44.
- [98] Shin SR, Bae H, Cha JM, Mun JY, Chen YC, Tekin H, Shin H, Farshchi S, Dokmeci MR, Tang S, Khademhosseini A. Carbon nanotube reinforced hybrid microgels as scaffolds materials for cell encapsulation. *ACS Nano* 2012;6:362–72.
- [99] Ayutseude J, Gandhi M, Sukigara S, Ye H, Hsu C, Gogotsi Y, Ko F. Carbon nanotube reinforced *Bombyx mori* silk nanofibers by the electrospinning process. *Biomacromolecules* 2006;7:208–14.
- [100] Yildirim ED, Yin X, Kalyani N, Sun W. Fabrication characterization and biocompatibility of single-walled carbon nanotube-reinforced alginate composite scaffolds manufactured using freeform fabrication technique. *J Biomed Mater Res* B 2008;87:406–14.
- [101] Hirata E, Uo M, Takita H, Akasaki T, Watari F, Yokoyama A. Multiwalled carbon nanotube-coating of 3D collagen scaffolds for bone tissue engineering. *Carbon* 2011;49:3284–91.
- [102] Khang D, Kim SY, Liu-Snyder P, Tayhas G, Palmore R, Durbin SM, Webster TJ. Enhanced fibronecin adsorption on carbon nanotube/poly(carbonate) urethane: independent role of surface nano-roughness and associated surface energy. *Biomaterials* 2007;28:4756–68.
- [103] Zhang H, Chen Z. Fabrication and characterization of electrospun PLGA/MWCNTs/hydroxyapatite biocomposite scaffolds for bone tissue engineering. *J Biact Compat Polym* 2010;25:241–59.
- [104] Armentano I, Dottori M, Puglia D, Kenny JM. Effects of carbon nanotubes (CNTs) on the processing and *in vitro* degradation of poly(DL-lactide-co-glycolide)/CNT films. *J Mater Sci Mater Med* 2008;19:2377–87.
- [105] Qian D, Dickey EC, Andrews R, Rantell T. Load transfer and deformation mechanisms in carbon nanotube-polystyrene composites. *Appl Phys Lett* 2000;76:2868–70.

- [106] Rege K, Ravikar NR, Kim DY, Schadler LS, Ajayan PM, Dordick JS. Enzyme-polymer-single walled carbon nanotube composites as biocatalytic films. *Nano Lett* 2003;3:829–32.
- [107] Shi X, Hudson JL, Spicer PP, Tour JM, Krishnamoorti R, Mikos AG. Injectable nanocomposites of single-walled carbon nanotubes and biodegradable polymers for bone tissue engineering. *Biomacromolecules* 2006;7:2237–42.
- [108] Zhang S, Grenfield MA, Mata A, Palmer LC, Bitton R, Mantei JR, Aparicio C, de la Cruz MO, Stupp SI. A self-assembly pathway to aligned monodomain gels. *Nat Mater* 2010;9:594–601.
- [109] Gutiérrez MC, Ferrer ML, del Monte F. Ice-templated materials: sophisticated structures exhibiting enhanced functionalities obtained after unidirectional freezing and ice-segregation-induced self-assembly. *Chem Mater* 2008;20:634–48.
- [110] Pate JW, Sawyer PN. Freeze-dried aortic grafts: a preliminary report of experimental evaluation. *Am J Surg* 1953;86:3–13.
- [111] Ross DN. Homograft replacement of the aortic valve. *Lancet* 1962;280:487.
- [112] Chen G, Ushida T, Tateishi T. Preparation of poly(L-lactic acid) and poly(DL-lactic-co-glycolic acid) foams by use of ice microparticulates. *Biomaterials* 2001;22:2563–7.
- [113] Ho MH, Kuo PY, Hsieh HJ, Hsien TY, Hou LT, Lai JY, Wang DM. Preparation of porous scaffolds by using freeze-extraction and freeze-gelation methods. *Biomaterials* 2004;25:129–38.
- [114] Kang HW, Tabata Y, Ikada Y. Fabrication of porous gelatin scaffolds for tissue engineering. *Biomaterials* 1999;20:1339–44.
- [115] Hsieh CY, Tsai SP, Wang DM, Chang YN, Hsieh HJ. Preparation of gamma-PGA/chitosan composite tissue engineering matrices. *Biomaterials* 2005;26:5617–23.
- [116] Ho MH, Wang DM, Liu CE, Hsieh CH, Tseng HC, Hsieh HJ. Analysis of freeze-gelation and cross-linking processes for preparing porous chitosan scaffolds. *Carbohydr Polym* 2007;67:124–32.
- [117] Daamen WF, Van Moerkirk HT, Hafmans T, Buttafoco L, Poot AA, Veerkamp JH, van Kuppevelt TH. Preparation and evaluation of molecularly-defined collagen-elastin-glycosaminoglycan scaffolds for tissue engineering. *Biomaterials* 2003;24:4001–9.
- [118] Dagalakis N, Flink J, Stasiklis P. Design of an artificial skin. Part III. Control of pore structure. *J Biomed Mater Res* 1980;14: 511–28.
- [119] Shalaby WSW, Peck GE, Park K. Release of dextromethorphan hydrobromide from freeze-dried enzyme-degradable hydrogels. *J Control Release* 1991;16:355–63.
- [120] Nardechchia S, Serrano MC, Gutiérrez MC, Ferrer ML, del Monte F. Modulating the cytocompatibility of tridimensional carbon nanotube-based scaffolds. *J Mater Chem B* 2013;1:3064–72.
- [121] Venkatesan J, Qian ZJ, Ryu B, Ashok Kumar N, Kim SK. Preparation and characterization of carbon nanotube-grafted-chitosan-natural hydroxyapatite composite for bone tissue engineering. *Carbohydr Polym* 2011;83:569–77.
- [122] Venkatesan J, Ryu B, Sudha PN, Kim SK. Preparation and characterization of chitosan-carbon nanotube scaffolds for bone tissue engineering. *Int J Biol Macromol* 2012;50:393–402.
- [123] Sweetman LJ, Moulton SE, Wallace GG. Characterization of porous freeze dried conducting carbon nanotube-chitosan scaffolds. *J Mater Chem* 2008;18:5417–22.
- [124] Mukai SR, Nishihara H, Tamon H. Preparation of resorcinol-formaldehyde carbon cryogel microhoneycombs. *Chem Commun* 2004;10:874–5.
- [125] Usui Y, Aoki K, Narita N, Murakami N, Nakamura I, Nakamura K, Ishigaki N, Yamazaki H, Horiuchi H, Kato H, Taruta S, Kim YA, Endo M, Saito N. Carbon nanotubes with high bone-tissue compatibility and bone-formation acceleration effects. *Small* 2008;4:240–6.
- [126] Bhattacharya S, Guillot S, Dabboue H, Tranchant JF, Salvat JP. Carbon nanotubes as structural nanofibers for hyaluronic acid hydrogel scaffolds. *Biomacromolecules* 2008;9:505–9.
- [127] Kwon SM, Kim HS, Jin HJ. Multiwalled carbon nanotube cryogels with aligned and non-aligned porous structures. *Polymer* 2009;50:2786–92.
- [128] Kawaguchi M, Fukushima T, Hayakawa T, Nakashima N, Inoue Y, Takeda S, Okamura K, Taniguchi K. Preparation of carbon nanotube-alginate nanocomposite gel for tissue engineering. *Dent Mater J* 2006;25:719–25.
- [129] Thongprachan N, Nakagawa K, Sano N, Charinpanitkul T, Than-thapanichakoon W. Preparation of macroporous solid foam from multi-walled carbon nanotubes by freeze-drying technique. *Mater Chem Phys* 2008;112:262–9.
- [130] Lewitus DY, Landers J, Branch JR, Smith KL, Callegari G, Kohn J, Neimark AV. Biohybrid carbon nanotube/agarose fibers for neural tissue engineering. *Adv Funct Mater* 2011;21:2624–32.
- [131] Dhandayuthapani B, Varghese SH, Aswathy RG, Yoshida Y, Maekawa T, Sakthikumar D. Evaluation of antithrombogenicity and hydrophilicity on Zein-SWCNT electrospun fibrous nanocomposite scaffolds. *Int J Biomater* 2012;1–10, 345029.
- [132] Rubenstein D, Han D, Goldgraben S, El-Gendi H, Gouma PI, Frame M. Bioassay chamber for angiogenesis with perfused explanted arteries and electrospun scaffolding. *Microcirculation* 2007;14: 723–37.
- [133] Rutledge SL, Shaw HC, Benavides JB, Yowell LL, Chen Q, Jacobs BW, Song SP, Ayres VM. Self assembly and correlated properties of electrospun carbon nanofibers. *Diam Relat Mater* 2006;15:1070–4.
- [134] Sharma Y, Tiwari A, Hattori S, Terada D, Sharma AK, Ramalingam M, Kobayashi H. Fabrication of conducting electrospun nanofibers scaffold for three-dimensional cells culture. *Int J Biol Macromol* 2012;51:627–31.
- [135] Zhang H, Liu J, Yao Z, Yang J, Pan L, Chen Z. Biomimetic mineralization of electrospun poly(lactic-co-glycolic acid)/multiwalled carbon nanotubes composite scaffolds in vitro. *Mater Lett* 2009;63:2313–6.
- [136] Zhang H. Electrospun poly(lactic-co-glycolic acid)/multiwalled carbon nanotubes composite scaffolds for guided bone tissue regeneration. *J Bioact Compat Polym* 2011;26:347–62.
- [137] Chang ZJ, Zhao X, Zhang QH, Chen DJ. Nanofibre-assisted alignment of carbon nanotubes in macroscopic polymer matrix via a scaffold-based method. *Express Polym Lett* 2010;4:47–53.
- [138] Liu F, Guo R, Shen M, Cao X, Mo X, Wang S, Shi X. Effect of the porous microstructures of poly(lactic-co-glycolic acid)/carbon nanotube composites on the growth of fibroblast cells. *Soft Mater* 2010;8:239–53.
- [139] Shao S, Zhou S, Li L, Li J, Luo C, Wang J, Weng J. Osteoblast function on electrically conductive electrospun PLA/MWCNTs nanofibers. *Biomaterials* 2011;32:2821–33.
- [140] Shao S, Li L, Yang G, Li J, Luo C, Gong T, Zhou S. Controlled green tea polyphenols release from electrospun PCL/MWCNTs composite nanofibers. *Int J Pharm* 2012;421:310–20.
- [141] Shao S, Li L, Yang G, Li J, Luo C, Gong T, Zhou S. Poly(acrylic acid)/poly(vinyl alcohol) compositions coaxially electrospun with poly(e-caprolactone) and multi-walled carbon nanotubes to create nanoactuating scaffolds. *Polymer* 2011;52:4736–43.
- [142] McKeon-Fischer KD, Flagg DH, Freeman JW. Coaxial electrospun poly(e-caprolactone)multiwalled carbon nanotubes and poly-acrylic acid/polyvinyl alcohol scaffold for skeletal muscle tissue engineering. *J Biomed Mater Res A* 2011;99:493–9.
- [143] Jin GZ, Kim M, Shin US, Kim HW. Effect of carbon nanotube coating of aligned nanofibrous polymer scaffolds on the neurite outgrowth of PC-12 cells. *Cell Biol Int* 2011;35:741–5.
- [144] Jin GZ, Kim M, Shin US, Kim HW. Neurite outgrowth of dorsal root ganglia neurons is enhanced on aligned nanofibrous biopolymer scaffold with carbon nanotube coating. *Neurosci Lett* 2011;501:10–4.
- [145] Kabiri M, Soleimani M, Shabani I, Futrega K, Ghaemi N, Ahvaz HH, Elahi E, Doran MR. Neural differentiation of mouse embryonic stem cells on conductive nanofiber scaffolds. *Biotech Lett* 2012;34:1357–65.
- [146] McCullen SD, Stevens DR, Roberts WA, Ojha SS, Clarke LI, Gorga RE. Morphological electrical and mechanical characterization of electrospun nanofibers mats containing multiwalled carbon nanotubes. *Macromolecules* 2007;40:997–1003.
- [147] McCullen SD, Stano KL, Stevens DR, Roberts WA, Monteiro-Riviere NA, Clarke LI, Gorga RE. Development optimization and characterization of electrospun poly(lactic acid) nanofibers containing multi-walled carbon nanotubes. *J Appl Polym Sci* 2007;105:1668–78.
- [148] Meng J, Kong H, Han Z, Wang C, Zhu G, Xie S, Xu H. Enhancement of nanofibrous scaffold of multiwalled carbon nanotubes/polyurethane composite to the fibroblasts growth and biosynthesis. *J Biomed Mater Res A* 2009;88:105–16.
- [149] Zomer Volpato F, Fernandes Ramos SL, Motta A, Migliarese C. Physical and in vitro biological evaluation of a PA 6/MWCNT electrospun composite for biomedical applications. *J Bioact Compat Polym* 2011;26:35–47.
- [150] Liao H, Qi R, Shen M, Cao X, Guo R, Zhang Y, Shi X. Improved cellular response on multiwalled carbon nanotube-incorporated electrospun polyvinyl alcohol/chitosan nanofibrous scaffolds. *Colloids Surf B* 2011;84:528–35.
- [151] Shokrgozar MA, Mottaghitalab F, Mottaghitalab V, Farokhi M. Fabrication of porous chitosan/poly(vinyl alcohol) reinforced single-walled carbon nanotube nanocomposites for neural tissue engineering. *J Biomed Nanotechnol* 2011;7:276–84.

- [152] MacDonald RA, Laurenzi B, Viswanathan G, Ajayan PM. Collagen-carbon nanotube composite materials as scaffolds in tissue engineering. *J Biomed Mater Res A* 2005;74:489–96.
- [153] Crouzier T, Nimmagadda A, Nollert MU, McFetridge PS. Modification of single walled carbon nanotube surface chemistry to improve aqueous solubility and enhance cellular interactions. *Langmuir* 2008;24:13173–81.
- [154] Tan W, Twomey J, Guo D, Madhavan K, Li M. Evaluation of nanostructural mechanical and biological properties of collagen-nanotube composites. *IEEE Trans Nanobiosci* 2010;9:111–20.
- [155] Tosun Z, McFetridge PS. A composite SWCNT-collagen matrix: characterization and preliminary assessment as a conductive peripheral nerve regeneration matrix. *J Neural Eng* 2010;7:66002.
- [156] Behan BL, DeWitt DG, Bogdanowicz DR, Koppes AN, Bale SS, Thompson DM. Single-walled carbon nanotubes alter Schwann cell behavior differentially within 2D and 3D environments. *J Biomed Mater Res A* 2011;96:46–57.
- [157] Chen CS, Soni S, Le C, Biasca M, Farr E, Chen EY, Chin WC. Human stem cell neuronal differentiation on silk-carbon nanotube composite. *Nanoscale Res Lett* 2012;7:126, 1–7.
- [158] Zou L, Liu J, Karakoti AS, Kumar A, Joung D, Li Q, Khondaker SI, Seal S, Zhai L. Ultralight multiwalled carbon nanotube aerogel. *ACS Nano* 2010;4:7293–302.
- [159] Firkowska I, Olek M, Pazos-Pérez N, Rojas-Chapana J, Giersig M. Highly ordered MWNT-based matrixes: topography at the nanoscale conceived for tissue engineering. *Langmuir* 2006;22:5427–34.
- [160] Boccaccini AR, Chircat F, Cho J, Bretcanu O, Roether JA, Novak S, Chen QZ. Carbon nanotube coatings on bioglass-based tissue engineering scaffolds. *Adv Funct Mater* 2007;17:2815–22.
- [161] Hirata E, Uo M, Nodasaka Y, Takita H, Ushijima N, Akasaka T, Watari F, Yokoyama A. 3D collagen scaffolds coated with multiwalled carbon nanotubes: initial cell attachment to internal surface. *J Biomed Mater Res B* 2010;93:544–50.
- [162] Luo Y, Wang S, Shen M, Qi R, Fang Y, Guo R, Cai H, Cao X, Tomás H, Zhu M, Shi X. Carbon nanotube-incorporated multilayered cellulose acetate nanofibers for tissue engineering applications. *Carbohydr Polym* 2013;91:419–27.
- [163] Zang R, Yang ST. Multiwalled carbon nanotube-coated polyethylene terephthalate fibrous matrices for enhanced neuronal differentiation of mouse embryonic stem cells. *J Mater Chem B* 2013;1:646–53.
- [164] Adeli H, Zein SHS, Tan SH, Akil HM, Ahmad AL. Synthesis characterization and biodegradation of novel poly(L-lactide)/multi-walled carbon nanotube porous scaffolds for tissue engineering applications. *Curr Nanosci* 2011;7:323–32.
- [165] Edwards SL, Church JS, Werkmeister JA, Ramshaw JAM. Tubular micro-scale multiwalled carbon nanotube-based scaffolds for tissue engineering. *Biomaterials* 2009;30:1725–31.
- [166] Lin C, Wang Y, Lai Y, Yang W, Jiao F, Zhang H, Ye S, Zhang Q. Incorporation of carboxylation multiwalled carbon nanotubes into biodegradable poly(lactic-co-glycolic acid) for bone tissue engineering. *Colloids Surf B* 2011;83:367–75.
- [167] Rizvi R, Kim JK, Naguib H. The effect of processing and composition on the properties of polylactide-multiwall carbon nanotube composites prepared by solvent casting. *Smart Mater Struct* 2010;19:094003, 1–8.
- [168] Meng J, Song L, Meng J, Kong H, Zhu G, Wang C, Xu L, Xie S, Xu H. Using single-walled carbon nanotubes nonwoven films as scaffolds to enhance long-term cell proliferation in vitro. *J Biomed Mater Res A* 2006;79:298–306.
- [169] Misra SK, Ansari TI, Valappil SP, Mohn D, Philip SE, Stark WJ, Roy I, Knowles JC, Salih Y, Boccaccini AR. Poly(3-hydroxybutyrate) multi-functional composite scaffolds for tissue engineering applications. *Biomaterials* 2010;31:2806–15.
- [170] Pan L, Pei X, He R, Wan Q, Wang J. Multiwall carbon nanotubes/polycaprolactone composites for bone tissue engineering application. *Colloids Surf B* 2012;93:226–34.
- [171] Shi X, Sitharaman B, Pham QP, Liang F, Wu K, Billups WE, Wilson LJ, Mikos AG. Fabrication of porous ultra-short single-walled carbon nanotube nanocomposite scaffolds for bone tissue engineering. *Biomaterials* 2007;28:4078–90.
- [172] Sitharaman B, Shi X, Walboomers XF, Liao H, Cuijpers V, Wilson LJ, Mikos AG, Jansen JA. In vivo biocompatibility of ultra-short single walled carbon nanotube/biodegradable polymer nanocomposites for bone tissue engineering. *Bone* 2008;43:362–70.
- [173] van der Zande M, Walboomers XF, Brännwall M, Olalde B, Jurado MJ, Álava JI, Jansen JA. Genetic profiling of osteoblast-like cells cultured on a novel bone reconstructive material consisting of poly-L-lactide carbon nanotubes and microhydroxyapatite in the presence of bone morphogenetic protein-2. *Acta Biomater* 2010;6:4352–60.
- [174] Kostarelos K. The long and short of carbon nanotube toxicity. *Nat Biotechnol* 2008;26:774–6.
- [175] Muller J, Huaux F, Moreau N, Misson P, Heilier JF, Delos M, Arras M, Fonseca A, Nagy JB, Lison D. Respiratory toxicity of multi-wall carbon nanotubes. *Toxicol Appl Pharmacol* 2005;207:221–31.
- [176] Osmund-McLeod MJ, Poland CA, Murphy F, Waddington L, Morris H, Hawkins SC, Clark S, Aitken R, McCall MJ, Donaldson K. Durability and inflammogenic impact of carbon nanotubes compared with asbestos fibres. *Part Fibre Toxicol* 2011;8:15, 1–18.
- [177] Murphy FA, Schinwald A, Poland CA, Donaldson K. The mechanism of pleural inflammation by long carbon nanotubes: interaction of long fibres with macrophages stimulates them to amplify pro-inflammatory responses in mesothelial cells. *Part Fibre Toxicol* 2012;9:8, 1–15.
- [178] Poland CA, Duffin R, Kinloch I, Maynard A, Wallace WAH, Seaton A, Stone V, Brown S, Macnee W, Donaldson K. Carbon nanotubes introduced into the abdominal cavity of mice show asbestos-like pathogenicity in a pilot study. *Nat Nanotechnol* 2008;3:423–8.
- [179] Donaldson K, Tran CL. An introduction to the short-term toxicology of respirable industrial fibres. *Mutat Res* 2004;553:5–9.
- [180] Mossman BT, Churg A. Mechanisms in the pathogenesis of asbestos and silicosis. *Am J Respir Crit Care Med* 1998;157:1666–80.
- [181] Nagai H, Okazaki Y, Chew SH, Misawa N, Yamashita Y, Akatsuka S, Ishihara T, Yamashita K, Yoshikawa Y, Yasui H, Jiang L, Ohara H, Takahashi T, Ichihara G, Kostarelos K, Miyata Y, Shinohara H, Toyokuni S. Diameter and rigidity of multiwalled carbon nanotubes are critical factors in mesothelial injury and carcinogenesis. *Proc Natl Acad Sci U S A* 2011;108:E1330–8.
- [182] Kolosnjaj-Tabi J, Hartman KB, Boudjemaa S, Ananta JS, Morgant G, Szwarc H, Wilson LJ, Moussa F. In vivo behavior of large doses of ultrashort and full-length single-walled carbon nanotubes after oral and intraperitoneal administration to Swiss mice. *ACS Nano* 2010;4:1481–92.
- [183] Muller J, Delos M, Panin N, Rabolli V, Huaux F, Lison D. Absence of carcinogenic response to multiwalled carbon nanotubes in a 2-year bioassay in the peritoneal cavity of the rat. *Toxicol Sci* 2009;110:442–8.
- [184] Pott F. Detection of mineral fibre carcinogenicity with the intraperitoneal test – recent results and their validity. *Ann Occup Hyg* 1995;39:771–9.
- [185] Takagi A, Hirose A, Nishimura T, Fukumori N, Ogata A, Ohashi N, Kitajima S, Kanno J. Induction of mesothelioma in p53+/– mouse by intraperitoneal application of multi-wall carbon nanotube. *J Toxicol Sci* 2008;33:105–16.
- [186] Sanchez VC, Weston P, Yan A, Hurt RH, Kane AB. A 3-dimensional in vitro model of epithelioid granulomas induced by high aspect ratio nanomaterials. *Part Fibre Toxicol* 2011;8:17, 1–18.
- [187] Tasis D, Tagmatarchis N, Georgakilas V, Prato M. Soluble carbon nanotubes. *Chem Eur J* 2003;9:4000–8.
- [188] Herrero MA, Lacerda L, Bianco A, Kostarelos K, Prato M. Functionalised carbon nanotubes: high biocompatibility with lack of toxicity. *Int J Nanotechnol* 2011;8:885–97.
- [189] Belyansкая L, Weigel S, Hirsch C, Tobler U, Krug HF, Wick P. Effects of carbon nanotubes on primary neurons and glial cells. *Neurotoxicology* 2009;30:702–11.
- [190] Li Z, Hulderman T, Salmon R, Chapman R, Leonard SS, Young SH, Shvedova A, Luster MI, Simenova PP. Cardiovascular effects of pulmonary exposure to single-wall carbon nanotubes. *Environ Health Perspect* 2007;115:377–82.
- [191] Wick P, Manser P, Limbach LK, Dettlaff-Weglikowska U, Krumeich F, Roth S, Stark WJ, Bruinink A. The degree and kind of agglomeration affect carbon nanotube cytotoxicity. *Toxicol Lett* 2007;168:121–31.
- [192] Liu Z, Davis C, Cai W, He L, Chenand X, Dai H. Circulation and long-term fate of functionalized biocompatible single-walled carbon nanotubes in mice probed by Raman spectroscopy. *Proc Natl Acad Sci U S A* 2008;105:1410–5.
- [193] Dong L, Joseph K, Witkowski KM, Craig M. Cytotoxicity of single-walled carbon nanotubes suspended in various surfactants. *Nanotechnology* 2008;19:255702, 1–5.
- [194] Bardi G, Tognini P, Ciofani G, Raffa V, Costa M, Pizzorusso T. Pluronic-coated carbon nanotubes do not induce degeneration of cortical neurons in vivo and in vitro. *Nanomedicine* 2009;5:96–104.
- [195] Dujardin E, Ebbesen TW, Krishnan A, Treacy MM. Purification of single-shell nanotubes. *Adv Mater* 1998;10:611–3.
- [196] Hamon MA, Chen J, Hu H, Chen Y, Itkis ME, Rao AM, Eklund PC, Haddon RC. Dissolution of single-walled carbon nanotubes. *Adv Mater* 1999;11:834–40.

- [197] Liu X, Hurt RH, Kane AB. Biodurability of single-walled carbon nanotubes depends on surface functionalization. *Carbon* 2010;48:1961–9.
- [198] Lobo AO, Ramos SC, Antunes EF, Marciano FR, Travá-Airoldi VJ, Corat EJ. Fast functionalization of vertically aligned multiwalled carbon nanotubes using oxygen plasma. *Mater Lett* 2012;70:89–93.
- [199] Lobo AO, Corat MAF, Antunes EF, Ramos SC, Pacheco-Soares C, Corat EJ. Cytocompatibility studies of vertically-aligned multi-walled carbon nanotubes: raw material and functionalized by oxygen plasma. *Mater Sci Eng C* 2012;32:648–52.
- [200] Lobo AO, Marciano FR, Ramos SC, MacHado MM, Corat EJ, Corat MAF. Increasing mouse embryonic fibroblast cells adhesion on superhydrophilic vertically aligned carbon nanotube films. *Mater Sci Eng C* 2011;31:1505–11.
- [201] Matsumoto K, Sato C, Nakai Y, Kitazawa A, Whitby RLD, Shimizu N. Neurite outgrowths of neurons with neurotrophin-coated carbon nanotubes. *J Biosci Bioeng* 2007;103:216–20.
- [202] Cheng W, Ding L, Lei J, Ding S, Ju H. Effective cell capture with tetrapeptide functionalized carbon nanotubes and dual signal amplification for cytosensing and evaluation of cell surface carbohydrate. *Anal Chem* 2008;80:3867–72.
- [203] Chen X, Tam UC, Czapinski JL, Lee GS, Rabuka D, Zettl A, Bertozzi CR. Interfacing carbon nanotubes with living cells. *J Am Chem Soc* 2006;128:6292–3.
- [204] Nimmagadda A, Thurston K, Nollert MU, McFetridge PS. Chemical modification of SWNT alters in vitro cell-SWNT interactions. *J Biomed Mater Res A* 2006;76:614–25.
- [205] Malarkey EB, Fisher KA, Bekyarova E, Liu W, Haddon RC, Parpura V. Conductive single-walled carbon nanotube substrates modulate neuronal growth. *Nano Lett* 2009;9:264–8.
- [206] Murugesan S, Park TJ, Yang H, Mousa S, Linhardt RJ. Blood compatible carbon nanotubes – nano-based neoproteoglycans. *Langmuir* 2006;22:3461–3.
- [207] Bottini M, Bruckner S, Niko K, Bottini N, Bellucci S, Magrini A, Bergamaschi A, Mustelin T. Multi-walled carbon nanotubes induce T lymphocyte apoptosis. *Toxicol Lett* 2006;160:121–6.
- [208] Tian F, Cui D, Schwarz H, Estrada GG, Kobayashi H. Cytotoxicity of single-wall carbon nanotubes on human fibroblasts. *Toxicol In Vitro* 2006;20:1202–12.
- [209] Singh R, Pantarotto D, Lacerda L, Pastorin G, Klumpp D, Prato M, Bianco A, Kostarelos K. Tissue biodistribution and blood clearance rates of intravenously administered carbon nanotube radiotracers. *Proc Natl Acad Sci U S A* 2006;93:3357–62.
- [210] Lacerda L, Ali-Boucetta H, Herrero MA, Pastorin G, Bianco A, Prato M, Kostarelos K. Tissue histology and physiology following intravenous administration of different types of functionalized multiwalled carbon nanotubes. *Nanomedicine* 2008;3:149–61.
- [211] Lacerda L, Soundararajan A, Singh R, Pastorin G, Al-Jamal K, Turton J, Frederik P, Herrero MA, Li S, Bao A, Emfietzoglou D, Mather S, Philips WT, Prato M, Bianco A, Goins B, Kostarelos K. Dynamic imaging of functionalized multi-walled carbon nanotube systemic circulation and urinary excretion. *Adv Mater* 2008;20:225–30.
- [212] Lacerda L, Herrero MA, Venner K, Bianco A, Prato M, Kostarelos K. Carbon-nanotube shape and individualization critical for renal excretion. *Small* 2008;4:1130–2.
- [213] Yang ST, Guo W, Lin Y, Deng XY, Wang HF, Sun HF, Liu YF, Wang X, Wang W, Chen M, Huang YP, Sun YP. Biodistribution of pristine single-walled carbon nanotubes in vivo. *J Phys Chem C* 2007;11:17761–4.
- [214] Schipper ML, Nakayama-Ratchford N, Davis CR, Kam NW, Chu P, Liu Z, Sun X, Dai H, Gambhir SS. A pilot toxicology study of single-walled carbon nanotubes in a small sample of mice. *Nat Nanotechnol* 2008;3:216–21.
- [215] van der Zande M, Sitharaman B, Walboomers XF, Tran L, Ananta JS, Veltien A, Wilson LJ, Alava JI, Heerschap A, Mikos AG, Jansen JA. In vivo magnetic resonance imaging of the distribution pattern of gadonanotubes released from a degrading poly(lactic-co-glycolic acid) scaffold. *Tissue Eng Part C* 2010;17:19–26.
- [216] Cai X, Paratala BS, Hu S, Sitharaman B, Wang LV. Multiscale photoacoustic microscopy of single-walled carbon nanotube-incorporated tissue engineering scaffolds. *Tissue Eng Part C* 2012;18:310–7.
- [217] Guillemot F, Mironov V, Nakamura M. Bioprinting is coming of age: report from the International Conference on Bioprinting and Biofabrication in Bordeaux (3B'09). *Biofabrication* 2010;2:01201.
- [218] Dorj B, Won JE, Kim JH, Choi SJ, Shin US, Kim HW. Robocasting nanocomposite scaffolds of poly(caprolactone)/hydroxyapatite incorporating modified carbon nanotubes for hard tissue reconstruction. *J Biomed Mater Res A* 2013;101:1670–81.
- [219] Willerth SM, Arendas KJ, Gottlieb DJ, Sakiyama-Elbert SE. Optimization of fibrin scaffolds for differentiation of murine embryonic stem cells into neural lineage cells. *Biomaterials* 2006;27:5990–6003.
- [220] Baharvand H, Hashemi SM, Kazemi Ashtiani S, Farrokhi A. Differentiation of human embryonic stem cells into hepatocytes in 2D and 3D culture systems in vitro. *Int J Dev Biol* 2006;50:645–52.
- [221] Garreta E, Genové E, Borrós S, Semino CE. Osteogenic differentiation of mouse embryonic stem cells and mouse embryonic fibroblasts in a three-dimensional self-assembling peptide scaffold. *Tissue Eng* 2006;12:2215–27.
- [222] Wang F, Weaver VM, Petersen OW, Larabell CA, Dedhar S, Briand P, Lupu R, Bissell MJ. Reciprocal interactions between beta1-integrin and epidermal growth factor receptor in three-dimensional basement membrane breast cultures: a different perspective in epithelial biology. *Proc Natl Acad Sci U S A* 1998;95:14821–6.
- [223] Doyle AD, Wang FW, Matsumoto K, Yamada KM. One-dimensional topography underlies three-dimensional fibrillar cell migration. *J Cell Biol* 2009;184:481–90.
- [224] Som C, Nowack B, Krug HF, Wick P. Toward the development of decision supporting tools that can be used for safe production and use of nanomaterials. *Acc Chem Res* 2013;46:863–72.